Ore Geology Reviews 118 (2020) 103213

Contents lists available at ScienceDirect

Ore Geology Reviews

journal homepage: www.elsevier.com/locate/oregeorev

Geology, mineralogy and stable isotope geochemistry of the Dzuunmod area in northern Mongolia: Constraints for gold ore genesis and sources

Yeongmin Kim[a,e], Insung Lee[a,*], Sodnom Oyungerel[a,b], Chikalov Altanzul[b,c], Luvsanchultem Jargal[b], Nak Kyu Kim[d]

[a] School of Earth and Environmental Sciences, Seoul National University, Seoul 08826, Republic of Korea
[b] School of Arts and Sciences, National University of Mongolia, Ulaanbaatar 14021, Mongolia
[c] Centerra Gold Mongolia, Ulaanbaatar, Mongolia
[d] Unit of Antarctic K-route Expedition, Korea Polar Research Institute, Incheon 21990, Republic of Korea
[e] Research Center for Geochronology and Isotope Analysis, Korea Basic Science Institute, Ochang 28119, Republic of Korea

ARTICLE INFO

Keywords:
Dzuunmod area
Orogenic gold
Stable isotope geochemistry
Ore genesis
Mongolia

ABSTRACT

The Dzuunmod area located in the North Khentii Gold belt (NKGB) of northern Mongolia includes lode gold deposits such as Gatsuurt, Sujigtei and Boroo with several minor gold deposits and occurrences. They show similar hydrothermal alteration assemblages (sericitic, siliceous and potassic) and ore mineral assemblages (pyrite and arsenopyrite with minor amount of galena, sphalerite and chalcopyrite). Gold occurs as native form and invisible gold in pyrite and arsenopyrite. The major sulfide minerals are separated into earlier non-auriferous stage and later auriferous grains containing invisible gold. Native gold postdates the major sulfide mineralization.

Gold and arsenic content of pyrite grains indicates that gold exists mainly as solid solution form (Au^{+1}) in the Gatsuurt and Boroo deposit whereas gold nanoparticle (Au^0) is present in the Sujigtei deposit. High Co/Ni and Mo/Ni ratios of pyrite grain suggest a post-sedimentary or hydrothermal origin and the ore-forming fluid was significantly affected by fluid-host rock interactions during mineralization processes.

Large variation of $\delta^{34}S$ values of pyrite and arsenopyrite from −2.6‰ to 17.2‰ indicates that sulfur seems to be mainly derived from a source with heterogeneous sulfur isotope composition, even though the role of magmatic sulfur as one of possible sulfur sources cannot be ruled out. Consistent with geological evidence, relatively positive $\delta^{34}S$ values suggest that sulfidation plays an important role for gold and sulfide precipitation. The calculated $\delta^{18}O$ values of hydrothermal fluid from the measured $\delta^{18}O$ values of quartz samples (from 14.7‰ to 17.7‰) indicate a metamorphic derivation of ore-forming fluid.

Gold mineralization processes in the Dzuunmod area seem to occur several times by multiple input of hydrothermal fluid and fluid-host rock interactions. The gold deposits in the Dzuunmod area are considered to be orogenic gold type influenced by fluid-host rock interactions in the deposit area.

1. Introduction

Orogenic gold deposit is one of main gold sources in the world and widely distributed in a long time range from Phanerozoic orogenic belts to Precambrian cratons (Goldfarb et al., 2001). It had been considered that they show consistent geological and geochemical characteristics including host rocks, alteration assemblages, fluid inclusion composition and oxygen isotope composition (Goldfarb et al., 2001 and references therein). An alteration assemblage of sericite, quartz, sulfide ± carbonate in greenschist-facies host rocks, low-salinity, CO_2-rich fluid and restricted range of $\delta^{18}O$ values (see the Samples and analytical method section for definition of notation) had been regarded as typical characteristics of this deposit type (Goldfarb et al., 2001, 2005). However, with an accumulation of recent studies on the orogenic gold deposits, there seem to be many uncertainties to interpret the fluid and metal sources mainly attributed to complicate geological settings of the orogenic gold deposit (Goldfarb and Groves, 2015 and references therein).

The trace element geochemistry of sulfide grains such as pyrite and arsenopyrite from various ore deposits is able to provide a valuable information about fluid and metal sources in the deposit area as well as in the source area (e.g., Clark et al., 2004; Koglin et al., 2010; Zhu et al.,

* Corresponding author.
E-mail address: insung@snu.ac.kr (I. Lee).

https://doi.org/10.1016/j.oregeorev.2019.103213
Received 27 March 2019; Received in revised form 6 August 2019; Accepted 2 November 2019
Available online 06 November 2019

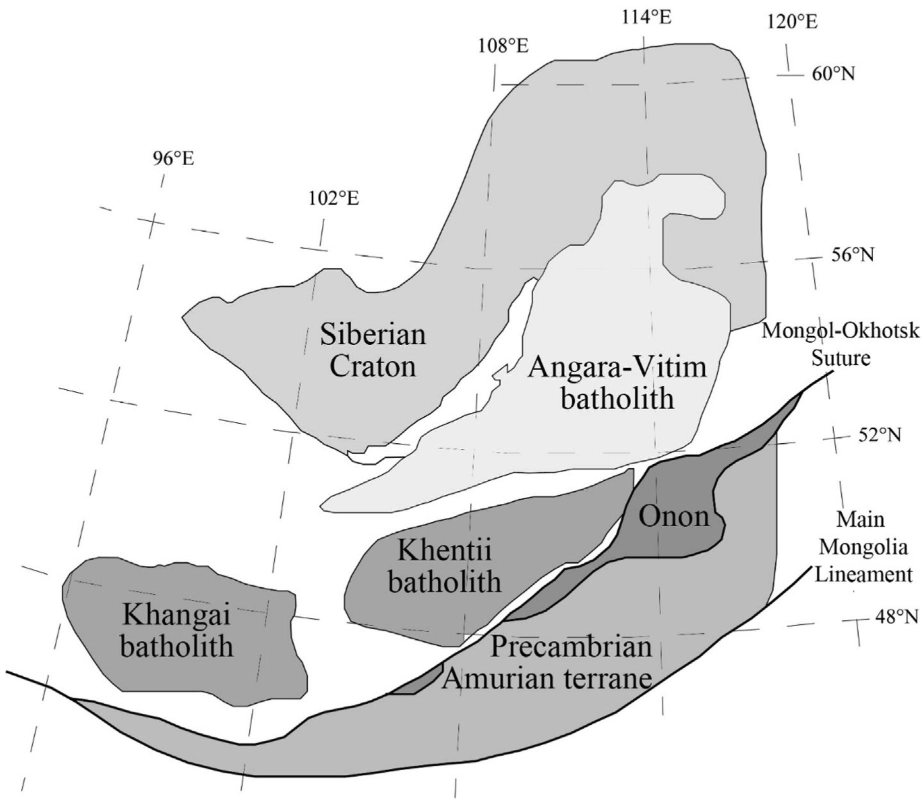

Fig. 1. Distribution of the Late Paleozoic to Early Mesozoic batholiths and belts in Mongolia and Russia (modified from Donskaya et al., 2013).

2011; Li et al., 2014; Niu et al., 2016; Yuan et al., 2018; Zhang et al., 2018). Trace element contents such as arsenic (As), cobalt (Co), nickel (Ni) and molybdenum (Mo) and their ratios like Co/Ni and Mo/Ni have been utilized to constrain the source characteristics and change of fluid composition during ore-forming processes in the gold deposit (Su et al., 2008; Sung et al., 2009; Yuan et al., 2018; Zhang et al., 2018). Especially, the As and gold (Au) content in the auriferous pyrite and arsenopyrite can be an useful indicator of gold occurrence form, estimated by an empirical gold solubility line as a function of As content (Reich et al., 2005).

Stable isotope measurement such as sulfur and oxygen has been pervasively applied to trace the fluid and sulfur sources and to understand the ore-forming processes in orogenic gold deposits for many decades (Kerrich, 1987, 1989; Nesbitt, 1991; Goldfarb and Groves, 2015). Most studies reported a narrow $\delta^{18}O$ range of auriferous hydrothermal fluids from 5‰ to 15‰ in the orogenic gold deposits (Kerrich, 1987; Bierlein and Crowe, 2000; Ding et al., 2016; Zhang et al., 2018). The $\delta^{18}O$ values of ore-forming fluid can be calculated from the $\delta^{18}O$ values of auriferous quartz vein and mineralization temperature estimated by fluid inclusion data (Vallance et al., 2004; Goldfarb and Groves, 2015; Wen et al., 2015; Hoefs, 2018) and/or arsenopyrite geothermometry (e.g., Koh et al., 1992; Zoheir, 2008; Deng et al., 2017). The uniform oxygen isotope composition of fluid favorably suggests the origination of ore-forming fluid from metamorphic devolatilization at depth (Goldfarb et al., 2005).

The S isotope ratio ($^{34}S/^{32}S$) of sulfide minerals in various ore deposits is indicative of the sulfur sources and the ore-forming processes (Ohmoto and Rye, 1979; Taylor, 1987; Rye, 2005; Seal, 2006). Especially, because it has been broadly accepted that gold is transported as bisulfide complexes in hydrothermal fluid under moderate salinities and temperature (e.g., Pokrovski et al., 2015), the $\delta^{34}S$ values accompanied with trace element composition of sulfides can be used to understand gold mineralization processes and to identify the sulfur sources in orogenic gold deposits (e.g., Hou et al., 2016; Ward et al., 2017; Yuan et al., 2018). The $\delta^{34}S$ values in in the orogenic gold deposit show an extremely large variation from −20‰ to 25‰ (Palin and Xu, 2000; Chang et al., 2008; Neumayr et al., 2008; Hodkiewicz et al., 2009; Ward et al., 2017; Xu et al., 2017; LaFlamme et al., 2018b; Ma et al., 2018; Yuan et al., 2018; Zhang et al., 2018). Ridley and Diamond (2000) argued that the $\delta^{34}S$ values of sulfide minerals in orogenic gold deposits reflect the evolution of sulfur isotope composition of sulfur species during transportation within hydrothermal fluid. This implies that the broad range of the $\delta^{34}S$ values in the orogenic deposits has been caused by not only multiple sources (e.g., Goldfarb et al., 2005; Goldfarb and Groves, 2015), but gold precipitation mechanisms such as fluid-rock interaction (e.g., Palin and Xu, 2000; Evans et al., 2006; Ward et al., 2017), phase separation by rapid pressure changes (e.g., Hodkiewicz et al., 2009), fluid mixing (e.g., LaFlamme et al., 2018a) and/or input of granitic magma (e.g., Neumayr et al., 2008; Hou et al., 2016).

The North Khentii Gold Belt (NKGB) is located in the Haraa terrane, northern Mongolia within the Mongol-Okhotsk orogenic belt and includes many lode and placer gold deposits with long history of gold production (Kampe and Gottesmann, 1966; Tumur et al., 1995; Gerel et al., 1999). The lode gold deposits contain Gatsuurt, Sujigtei, Boroo, Ereen and Ulaanbulag deposit with several gold occurrences such as Balj, Biluut, Urt and Baavgait (Dejidmaa, 1996), compiled to the Dzuunmod area. The Boroo and the Gatsuurt deposit have been estimated to have large tonnage, which is more than 50 Au tons, whereas the other deposits are lack of economic significance (Dejidmaa, 1996; Gerel et al., 1999). These deposits have been described to show similar geological and geochemical characteristics such as host rocks, alteration assemblages, mineralization types by several previous studies, classified as an orogenic gold deposit (Kampe and Gottesmann, 1966; Tumur et al., 1995; Cluer et al., 2005; Hendry et al., 2006; Goldfarb et al., 2014; Khishgee et al., 2014; Khishgee and Akasaka, 2015). Compared to mineralogical and petrological studies, there have been few researches about stable isotope compositions of the Dzuunmod area.

Here, we reported the trace element composition of auriferous pyrite and arsenopyrite, $\delta^{34}S$ values of sulfide minerals, and $\delta^{18}O$ values of the quartz grains with mineralogical and petrological observation of ore and gangue minerals (1) to identify the geological and geochemical features of the deposit, (2) to constrain the fluid and sulfur sources related to the gold mineralization, and (3) to understand the ore-forming processes in the Dzuunmod area.

2. Geological setting

2.1. Regional geological setting

Central Asian Orogenic Belt (CAOB) is one of the largest orogenic accretionary complexes on Earth and contains lots of Phanerozoic orogenic gold deposits (Yakubchuk et al., 2005; Goldfarb et al., 2014). Mongol-Okhotsk orogenic belt (or suture), part of the CAOB, was located among Siberian Craton and several granitoid batholiths in Late Paleozoic to Early Mesozoic period (Fig. 1) (e.g., Zorin, 1999; Parfenov et al., 2001; Badarch et al., 2002). Even though there have been still some debates on the formation and closure time of the Mongol-Okhotsk Ocean, its development was linked to the tectonic evolution of North and Central Mongolia (Şengör et al., 1993; Sengor and Natal'In, 1996; Zorin, 1999; Parfenov et al., 2001; Tomurtogoo et al., 2005; Bussien et al., 2011; Donskaya et al., 2013).

The Khangai-Khentii basin in the north-central Mongolia was the part of the Mongol-Okhotsk Ocean and separated by a northwest fault system into Khangai basin in the west and Khentii basin in the east (Fig. 2) (Zonenshain et al., 1990; Sengor and Natal'In, 1996; Badarch et al., 2002; Kelty et al., 2008). It mainly consists of Devonian to Carboniferous turbidite sequence intruded by Mesozoic igneous rocks (Badarch et al., 2002; Tomurtogoo et al., 2005; Kelty et al., 2008). In the northern range of the Khentii basin, the Haraa terrane bounded by the Yeroogol and the Bayangol fault systems occurs (Fig. 2). The terrane was forearc/backarc basin and mostly consists of Middle-Late Cambrian to Early Ordovician greenschist metasedimentary rocks such as sandstone, siltstone, argillite, phyllite, schist with minor amount of conglomerate and tuff, which is intruded by Ordovician to Devonian igneous rocks (Kampe and Gottesmann, 1966; Tumur et al., 1995; Badarch et al., 2002).

The NKGB is hosted within the Haraa terrane (Fig. 2) and considered to form during the closure of the Mongol-Okhotsk Ocean during Mesozoic period (Cluer et al., 2005). The NKGB is bounded by two left-lateral fault systems, which is the Bayangol fault in the northwest and Yeroogol fault system in the southeast with SW-NE trending (Fig. 2). Four major lithological units comprise the NKGB (Tumur et al., 1995; Kotlyar et al., 1998; Gerel et al., 1999; Cluer et al., 2005; Hendry et al., 2006): (1) Late Proterozoic to Early Paleozoic metasedimentary rocks of the Yeroo Group (greenschist metamorphic rocks) and Haraa Group (sandstone, shale, siltstone, conglomerate, phyllite and schist) and late Ordovician Boroogol Complex (granitoids); (2) Dzuunmod subvolcanic Complex (rhyolite porphyry, tuffaceous andesite lava and breccia) and sedimentary rocks (shale, sandstone and conglomerate); (3) Late Triassic to Early Jurassic granite Complex; and (4) Late Mesozoic coal-bearing sedimentary rocks and conglomerates.

2.2. Geological setting of Dzuunmod area

In the Dzuunmod area, Middle to Late Cambrian Haraa Group, Middle to Late Ordovician Boroogol Complex and Early Ordovician Dzuunmod subvolcanic Complex are widely distributed, hosting most gold deposits (Fig. 3) (Tumur et al., 1995; Kotlyar et al., 1999; Cluer

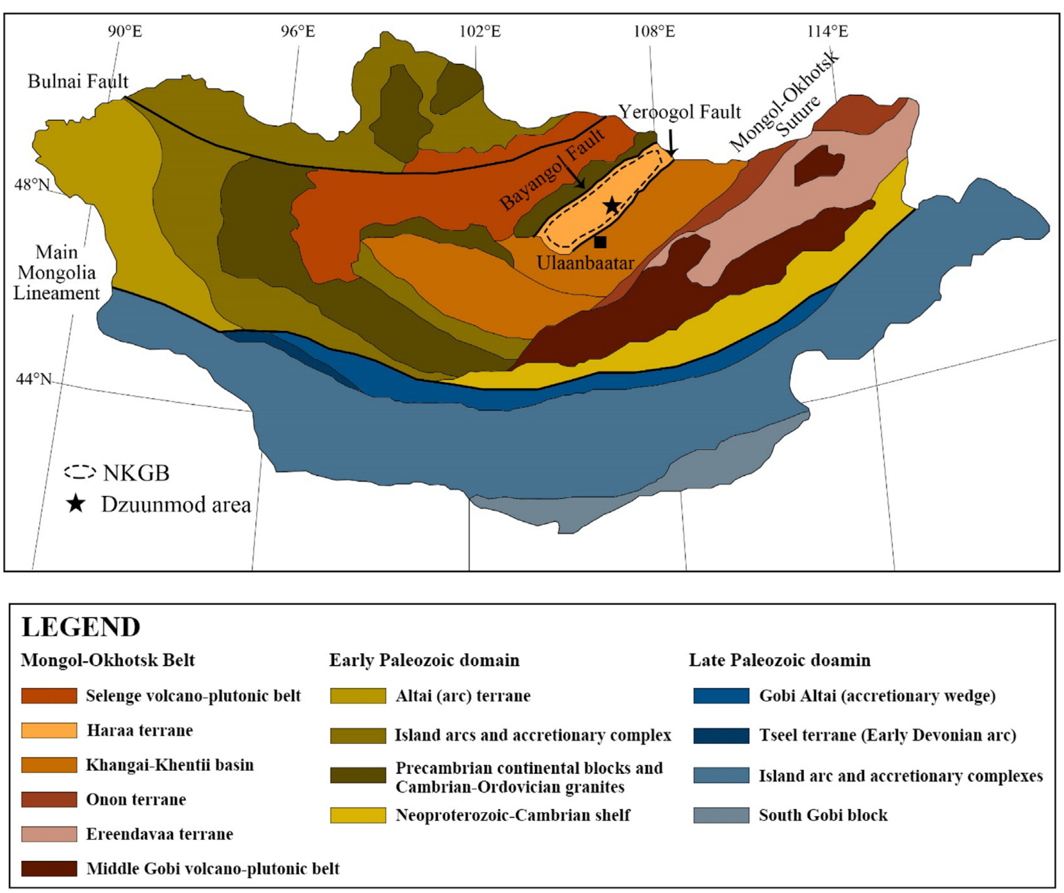

Fig. 2. Simplified tectonostratigraphic map of Mongolia (modified after Badarch et al., 2002; Bussien et al., 2011).

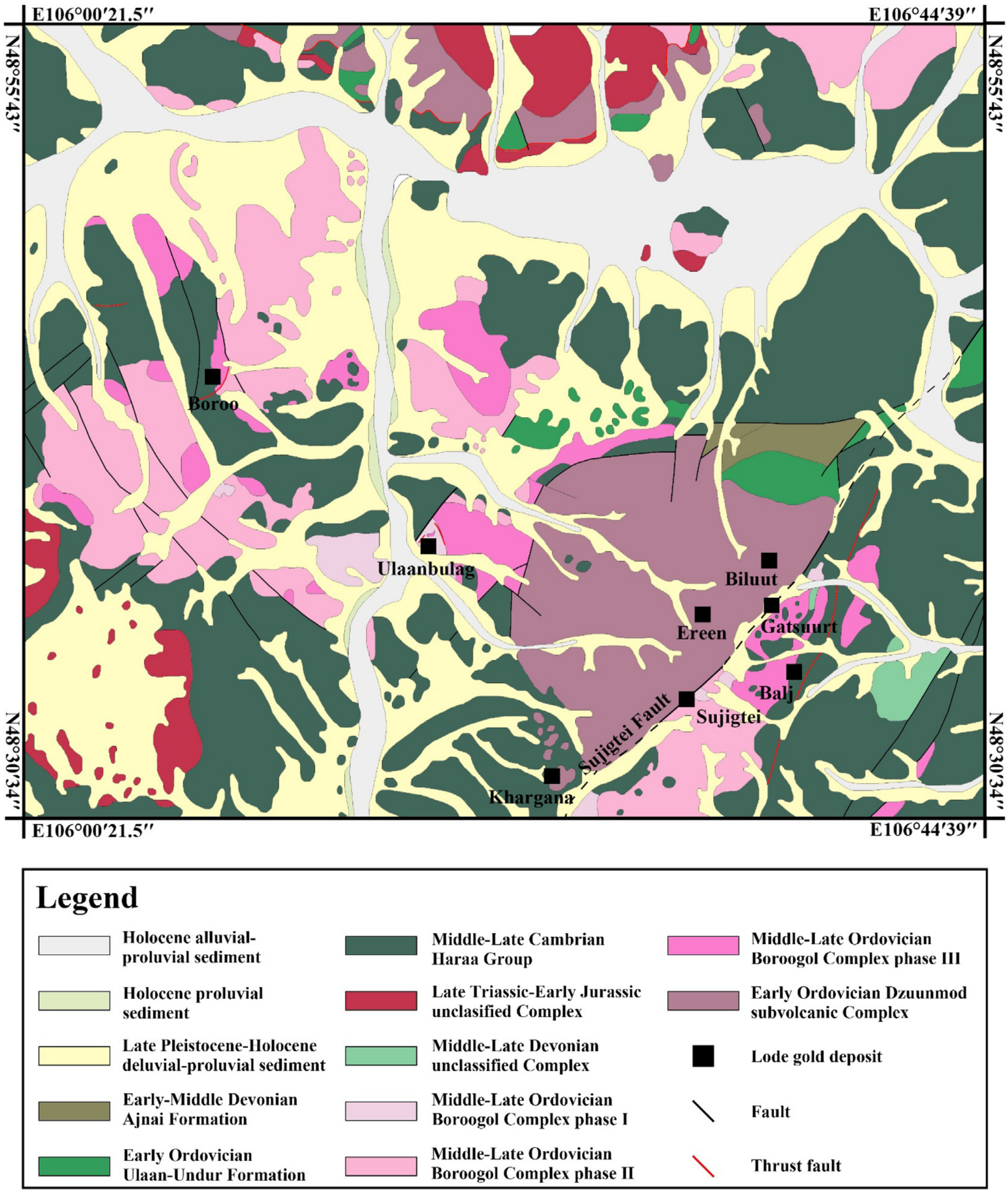

Fig. 3. Geological map of the North Khentii Gold Belt (NKGB) in northern Mongolia and the distribution of major lode deposit in the area (modified from Khishgee and Akasaka, 2015). The age of Dzuunmod subvolcanic Complex is still controversial. See the text for detail.

et al., 2005; Hendry et al., 2006). The Boroogol Complex is subdivided into three phases: medium grained gabbro, diorite and quartz-diorite (Phase I), medium-coarse grained granodiorite (Phase II), and medium-coarse grained granite and leucogranite (Phase III). Semi-circular Dzuunmod subvolcanic Complex is usually bounded with other rocks by faults (Fig. 3) and composed of rhyolite, rhyolite porphyry and tuff breccia (Kampe and Gottesmann, 1966; Tumur et al., 1995; Kotlyar et al., 1999). The metasedimentary rocks (calcareous sandstone, siltstone and slate) of the Middle-Late Cambrian to Early Ordovician Haraa Group was intruded by multiple phases of the Middle to Late Ordovician Boroogol Complex (Kampe and Gottesmann, 1966; Tumur et al., 1995; Cluer et al., 2005; Hendry et al., 2006). Volcanic rocks of Early Ordovician Ulaan-Undur formation are located in north and north-west Dzuunmod area (Tumur et al., 1995). Small intrusive bodies and dykes including unaltered medium-grained leucogranite, monzodiorite and diorite occur in the central part of the Dzuunmod area (Tumur et al., 1995), which is cut by Dzuunmod subvolcanic Complex (Altanzul et al., 2018). Early to Middle Devonian Ajnai Formation is composed of sedimentary rocks such as sandstone, conglomerate and siltstone (Tumur et al., 1995). The Ajnai Formation is bounded with the Ulaan-Undur Formation on the northern side of the Dzuunmod subvolcanic Complex (Fig. 3). Quaternary alluvial, deluvial and proluvial sediments are widely distributed on the valleys and its tributaries in the Dzuunmod area (Fig. 3).

Gold deposits in the Dzuunmod area are located along the NE-trending fault (Tumur et al., 1995; Cluer et al., 2005; Hendry et al., 2006). The Gatsuurt and the Sujigtei deposit in the Dzuunmod area are located on the Sujigtei fault (Fig. 3), which is a branch of the Yeroogol fault system. The Sujigtei fault, high-angle fault (oriented 40°) with NE-trending, is a boundary between the Dzuunmod subvolcanic Complex and the Boroogol Complex (Kampe and Gottesmann, 1966; Tumur et al., 1995; Altanzul et al., 2018). Displacement along the fault seems to be 800 m with the left-lateral movement. Because tectonic clay (or fault gouge) and clay-mylonitic alteration zone is very narrow, the

Sujigtei fault is suggestive to play a second or higher order role in the fault system relative to the Yeroogol fault (Hendry et al., 2006). However, the Sujigtei fault and parallel faults are one of major structural elements controlling the distribution of gold mineralization in the Gatsuurt and Sujigtei deposit (Altanzul et al., 2018). The Boroo deposit is also controlled by NE-trending thrust fault, called as Boroo fault and mainly hosted by the Haraa Group and Boroogol Complex (Cluer et al., 2005; Khishgee and Akasaka, 2015). Ore zones extend along the thrust fault system (Cluer et al., 2005; Khishgee and Akasaka, 2015).

2.3. Ages of the deposits in the Dzuunmod area

The U-Pb isotope compositions of zircon grains from five samples in Dzuunmod area were measured by SHIRMP (Altanzul et al., 2018). A weighted mean of $^{206}Pb/^{238}U$ concordant age is 476.2 ± 3.0 Ma (granite), 473.1 ± 3.8 Ma (diorite porphyry), and 471.4 ± 2.7 Ma (granite) in the Gatsuurt deposit and 467.0 ± 3.8 Ma (diorite) and 464.6 ± 4.9 Ma (granodiorite) in the Ulaanbulag deposit. First three and the other ages are corresponding to early and middle Ordovician, respectively. The U-Pb ages of the Gatsuurt deposit area are slightly older than those of the Ulaanbulag deposit area, although the error range (1σ) of them overlaps. This means that there is small but distinct difference of intrusion timing between the Gatsuurt and Ulaanbulag deposit area. Previous study on the U-Pb age dating of ore-bearing granite in the Boroo deposit reported 452.2 ± 3.9 Ma and 441.9 ± 6.6 Ma U-Pb age of zircon, corresponding to the late Ordovician period (Hou et al., 2010). These slightly younger U-Pb ages indicate that the intrusion of the Boroogol Complex seems to occur about 20–30 Ma earlier in the Boroo deposit area than Gatsuurt and Ulaanbulag deposit area.

It is suggested that there was temporal variation of the intrusion timing of the Boroogol Complex in the Dzuunmod area. In the study area, the Gatsuurt and the Boroo deposit are located in the most southeastern and northwestern part, whereas the Ulaanbulag deposit is positioned in the middle of them (Fig. 3). The U-Pb age of zircon grains is getting younger toward from the Gatsuurt deposit of the early Ordovician to the Boroo deposit area in the late Ordovician. This indicates that the Boroogol Complex intruded earlier in the Gatsuurt deposit area and occurred in the Ulaanbulag and the Boroo deposit area successively.

In contrast to the consistent age of Boroogol Complex, the absolute age of the Dzuunmod subvolcanic Complex such as rhyolite and rhyolite porphyry is still controversial. Earlier studies reported the K-Ar ages of rhyolite porphyry in the Dzuunmod area as 295 ± 20 Ma for whole rock and 305 ± 30 Ma for biotite (Kampe and Gottesmann, 1966). Also, Baasandolgor (2003) reported the Rb-Sr whole rock age of 288.4 ± 14 Ma for rhyolite porphyry in the Dzuunmod area, which is corresponding to Early Permian. However, several recent studies reported quite different U-Pb zircon age of rhyolite porphyry, diorite porphyry and granite samples in the Dzuunmod area (Khishgee, 2015; Onon and Tsukada, 2017), which is mostly corresponding to Ordovician. The U-Pb zircon ages of rhyolite porphyry are 485.5 ± 4.8 Ma (Khasmaral, unpublished data), and from 424 ± 18 Ma to 542 ± 16 Ma (Onon and Tsukada, 2017). Except two end values (424 ± 18 Ma and 542 ± 16 Ma), a weighted mean of $^{206}Pb/^{238}U$ concordant age of the other seven analyses is 457.1 ± 6.9 Ma (Onon and Tsukada, 2017). The U-Pb zircon age of diorite porphyry reported by Khishgee (2015) is 465.4 ± 3.0 Ma. Also, Altanzul et al. (2018) reported the U-Pb zircon ages of diorite porphyry dike (473.1 ± 3.8 Ma) and small stock granite (475.2 ± 6.1 Ma) cut by the Dzuunmod subvolcanic Complex. Even though the measured U-Pb zircon age of small stock granite is slightly deviated (MSWD = 5.5), these analyses results with geological relationship indicate the Early Ordovician age of the Dzuunmod subvolcanic Complex (Altanzul et al., 2018)

Cluer et al. (2005) reported the $^{40}Ar/^{39}Ar$ age dating results of hydrothermal alteration minerals such as sericite and muscovite in the Gatsuurt and the Boroo deposit. The $^{40}Ar/^{39}Ar$ age of the Gatsuurt deposit is *ca.* 178 Ma corresponding to early Jurassic, while the mineralization age of the Boroo deposit range from 208.3 ± 1.9 Ma to 186.2 ± 1.6 Ma of late Triassic to early Jurassic period (Cluer et al., 2005). Because the mineralization of gold is related to the hydrothermal alteration (e.g., sericitic alteration) in the study area, it seems to interpret that the hydrothermal alteration age represents the mineralization age. Therefore, the intrusion of the Boroogol Complex and gold mineralization event occurred in the significantly different period, indicating that the completely different tectonic or geological events were related to the intrusion and mineralization processes.

3. Samples and analytical methods

More than 100 ore and host rocks samples were collected from the drill core for microscopic observation, trace element and stable isotope analysis. Representative polished ore sections and thin sections were made for mineral identification by microscope and Electron Probe Micro Analyzer (EPMA). Sulfide and quartz grains were separated from the crushed rock samples by hand-picking method for sulfur and oxygen isotope analysis.

Trace element composition of ore minerals was analyzed by EPMA (JEOL, JXA-8530F PLUS) in the Center for research facilities of Gyeongsang National University, Korea. Accelerating voltages were 15 kV and beam size was 5 μm.

The sulfide minerals were prepared as a powder and put into a 3.5 × 5 mm tin-foil cup. The combustion was conducted in the tube packed with reagent materials of quartz wool, quartz chips and ultra-high purity Cu wire under the 1030 °C in the Elemental Analyzer (EA). The sulfur isotope composition (^{32}S and ^{34}S) was measured by Continuous Flow (CF)-EA-IRMS (IsoPrime-EA) at the School of Earth and Environmental Sciences (SEES), Seoul National University. The standard material (IAEA S-1) was bracketed within the samples. The data were calculated by linear regression of the standard and the sulfur isotope composition of the samples is expressed using δ-notation relative to the Vienna-Canyon Diablo Troilite (V-CDT) as follows:

$$\delta^{34}S_{(V-CDT)} = [(^{34}S/^{32}S)_{sample} - (^{34}S/^{32}S)_{(V-CDT)}]/(^{34}S/^{32}S)_{(V-CDT)}$$

Typically, $\delta^{34}S_{(V\text{-}CDT)}$ values are reported in per mil (‰, parts per thousand) which means that δ-value obtained by above equation are then multiplied by 1000. Samples and standards were analyzed in duplicate, and the external reproducibility for long-term analyses was better than ± 0.2‰.

The quartz grains were hand-picked from crushed ore samples and prepared as a fine-grain. The oxygen isotope composition of quartz grains was analyzed using a CO_2-laser BrF_5 fluorination system installed at Korea Polar Research Institute (KOPRI). The system is composed of four major parts: (1) reaction chamber, (2) 25 W CO_2 laser, (3) purification line and (4) mass spectrometer (MAT 253 plus, Thermo Fisher Scientific) controlled by ISODAT 3.0 software. The detail explanation of method for oxygen isotope analysis is described in Kim et al. (2019). The external reproducibility of oxygen isotope analysis is better than ± 0.05‰ (2σ) for $\delta^{18}O$ based on repetitive analyses of obsidian in-house standard and expressed using δ-notation relative to the Vienna Standard Mean Ocean Water (V-SMOW) as follows:

$$\delta^{18}O_{(V-SMOW)} = [(^{18}O/^{16}O)_{sample} - (^{18}O/^{16}O)_{(V-SMOW)}]/(^{18}O/^{16}O)_{(V-SMOW)}$$

Typically, $\delta^{18}O_{(V\text{-}SMOW)}$ values are reported in per mil (‰, parts per thousand) which means that δ-value obtained by above equation are then multiplied by 1000.

4. Alteration and mineralization characteristics of the Dzuunmod area

In the Dzuunmod area, six alteration types are distinctly observed including sericitic, siliceous, potassic, propylitic, carbonatic and argillic alteration, indicating the multiple events of hydrothermal alteration. The gold mineralization is associated with first three alteration types. The sericitic alteration consists of sericite, quartz and pyrite assemblage and is mainly related to a mineralization of low-sulfide with gold-quartz vein style. This assemblage intensely occurs in rhyolite, granite and even metasedimentary rocks. The siliceous alteration mainly develops as quartz veinlets, stockwork and massive style. The potassic alteration is divided into massive core coincident with potential gold mineralization and peripheral alteration. In the Gatsuurt deposit, the occurrence of the potassic alteration shows spatial variation in accordance with the distance from the central part of the deposit, which is associated with gold mineralization processes. The massive core alteration is coincident with potential gold mineralization and confined to the central part of the Gatsuurt deposit and nearby Sujigtei fault. The peripheral alteration is hosted by volcanic rocks, making the outer boundary of the Main zone of the Gatsuurt deposit.

There are three types of major gold mineralization in the Dzuunmod area: disseminated/stockwork, quartz vein and silicified. First type occurs in granite and rhyolite porphyry with the sericitic and potassic alteration assemblages accompanied by pyrite and arsenopyrite as a major sulfide mineral. Gold exists as invisible form in the sulfide grain. The quartz vein type includes major sulfide minerals and native gold with minor sphalerite and galena. The silicified type is subdivided into pervasive quart silicified zone (PQSZ), black quartz zone (BQZ) and normal silicified zone. The PQSZ consists of medium to coarse-grained quartz with visible gold, fine-grained arsenopyrite and pyrite. The BQZ occurs only in the Central zone of the Gatsuurt deposit and contains very fine-grained quartz, pyrite, arsenopyrite and minor amount of chalcopyrite, tetrahedrite and stibnite. The normal silicified zone is composed of fine-grained quartz, sericite with few sulfide minerals. The geological characteristics of major gold deposits and occurrences in study area are summarized in Table 1.

Based on the common alteration and mineralization characteristics of the Dzuunmod area, each deposit and occurrence is described in the following section. Three major deposits in the Dzuunmod area, Gatsuurt, Sujigtei and Boroo, individually form Sections 4.1 to 4.3 while other barren deposits and occurrences including Ereen, Ulaanbulag, Khargana, Balj and Biluut are combined into Section 4.4 together. Then, the paragenetic sequences of quartz and ore minerals in the Gatsuurt and the Boroo deposit followed in Section 4.5.

4.1. Gatsuurt deposit

The Gatsuurt deposit (Fig. 4a), first discovered in 1998, is mainly hosted by granitoids (Boroogol Complex), metasedimentary rocks (Haraa Group) and volcanic rocks of rhyolite and rhyolite porphyry (Dzuunmod subvolcanic Complex) (Fig. 5a and b) bounded by the left-lateral Sujigtei fault (Fig. 4-b and c). The Gatsuurt deposit is subdivided into Main zone, Central zone, South Slope and GT60 (Fig. 4a) and the style and magnitude of gold mineralization varies depending on the host rocks. The Main zone consists of sericitic and siliceous alteration assemblages in sulfidized rhyolite porphyry with disseminated/stockwork and quartz vein mineralization types (Fig. 5b). Pyrite and arsenopyrite are major sulfide minerals with quartz, sericite and carbonate as a major gangue mineral. The Central zone, South Slope and GT60 is hosted by Boroogol Complex consisting of hornblende-biotite granite, granodiorite and diorite (Fig. 5a and c) and metasedimentary rocks of Haraa Group (Fig. 5d). The disseminated/stockwork type occurs within the Boroogol Complex of the Central zone while silicified mineralization along the fault and quartz vein type exist in the Haraa Group. The South Slope zone is located in Southeast side of the Central

Table 1
Summary of geological characteristics of gold deposits and occurrences in the Dzuunmod area.

Deposit	Host rocks	Structure	Alteration Assemblage	Ore type	Major sulfide ore minerals
Gatsuurt	Granite, Sandstone, Diorite, Rhyolite	Sujigtei fault-steep	Siliceous, potassic, sericitic, carbonatic	sulfide zone, quartz vein, silica	Py, Asp, Cpy, Sph, Gal
Sujigtei	Granite	Sujigtei fault-steep	Siliceous, sericitic, potassic	Quartz vein	Py, Asp, Gal, Cpy
Boroo	Granite, Sandstone, Diorite	Boroo fault-gentle dipping	Siliceous, potassic, sericitic, carbonatic	sulfide zone, quartz vein	Py, Asp, Cpy, Sph, Gal
Ereen	Rhyolite	Gentle dipping	Siliceous, sericitic, potassic	Quartz vein	Py, Asp, Cgal, Cpy
Ulaanbulag	Granite, Sandstone, Diorite	Ulaanbulag fault-gentle dipping	Siliceous, potassic, sericitic, carbonatic	sulfide zone, quartz vein	Py, Asp, Gal, Sph
Balj	Sandstone	Balj fault-gentle dipping	Siliceous, sericitic, carbonatic	Quartz vein	Py, Asp
Biluut	Rhyolite	Gentle dipping	Siliceous, potassic, sericitic	quartz vein, sulfide zone	Py, Asp
Khargana	Rhyolite	Gentle dipping	Siliceous, sericitic	quartz vein	Py, Asp, Cpy

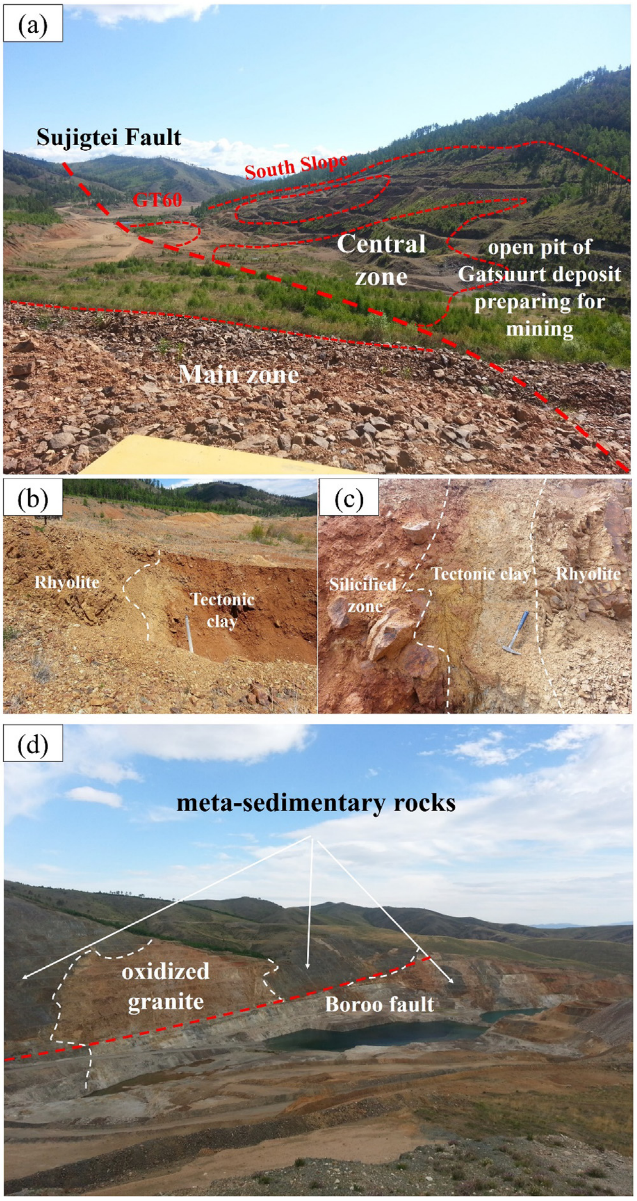

Fig. 4. Field photographs of ore deposits in the Dzuunmod area. (a) View of Gatsuurt deposit with Sujigtei fault, (b) & (c) host rocks, tectonic clay and siliceous rocks in the Gatsuurt deposit, and (d) view of open-pit mine in Boroo deposit.

zone and the host rock is granite with siliceous, sericitic and potassic alteration. The GT60 is placed in Northwest side of the Central zone along the Sujigtei fault (Fig. 4a) with disseminated/stockwork mineralization in granite and diorite affected by siliceous, sericitic and potassic alteration assemblages.

The sulfidized granite of Boroogol Complex mainly consists of plagioclase, K-feldspar and quartz with minor amount of biotite (Fig. 5a). The small mineral grains occur along the fractures within the rock where quartz and carbonate veins are developed with the width less than 2 mm (Fig. 5a). The rhyolite porphyry of the Dzuunmod subvolcanic Complex are separated into quartz and plagioclase phenocryst (10–15%) and groundmass (85–90%) showing the replacement of plagioclase to clay mineral, sericite and carbonate (Fig. 5b). The siliceous and carbonatic alteration occur with quartz and carbonate veins within the rock (Fig. 5b). Diorite is composed of plagioclase, hornblende and minor amount of biotite with rare quartz and altered by later carbonatic and sericitic alterations (Fig. 5c). The carbonatic alteration divides the rock into several part and carbonate occurs along the fractures within the diorite (Fig. 5c). The sulfidized sandstone of Haraa Group is extensively exposed to metamorphic processes causing recrystallization of most minerals (Fig. 5d). Plagioclase fragments are usually altered to sericite and minor amount of carbonate.

Gold mineralization of the Gatsuurt deposit includes all three mineralization types. The disseminated/stockwork type is observed in granite with an assemblage of quartz, sericite and K-feld spar. The major sulfide minerals are pyrite and arsenopyrite (Fig. 6-a and b) and quartz, sericite and carbonate occur as a gangue mineral. The silicified type including all three sub-classified types occurs only in the Central zone and consists of fine-grained quartz with minor sericite and disseminated sulfide minerals (Fig. 5e). Especially, the BQZ is uniquely detected in the Central zone. Pyrite and arsenopyrite are major sulfide minerals and gold grain occurs both as native form (Fig. 6c) and invisible gold in the sulfide minerals. The quartz vein type occurs in most volcanic rocks and granitoids such as rhyolite and granite (Fig. 5f) altered by sericite alteration. Quartz veins contain major sulfide minerals and native gold with minor amount of sphalerite and galena (Fig. 6c, d and e). Pyrite and arsenopyrite occur with minor amount of galena, sphalerite and native gold in quartz vein type ores (Fig. 6d and e) whereas major and minor ore minerals occur separately in the other types, indicating that they formed at different mineralization stage.

4.2. Sujigtei deposit

The Sujigtei deposit, 7 km southwest away from the Gatsuurt deposit (Fig. 3), was first discovered in early 20th century and has been mined as several small underground mines along the fault. The main host rock for gold-bearing quartz vein and disseminated/stockwork mineralization is granite (Fig. 5g and h) whereas rhyolite and rhyolite porphyry are usually barren. The altered granite in the Sujigtei deposit consists of quartz, plagioclase and K-feldspar with a minor amount of altered biotite and muscovite showing intensive sericitic alteration with quartz veinlet (Fig. 5g). The sulfidized rhyolite is composed of quartz, plagioclase and K-feldspar phenocrysts (20–25%) with 75–80% groundmass. The NE-trending faults with N45E/85SE show no apparent displacement and the largest lode structure is referred to as 'vein-1'. The main fault zone is composed of fault gouge and siliceous altered materials and important gold mineralization is associated with the fault. The major sulfide minerals are pyrite and arsenopyrite with minor galena and Cu-bearing minerals such as chalcopyrite, bornite, covellite and chalcocite (Fig. 6f). In addition, very tiny native gold grains are observed within pyrite grain (Fig. 6g).

4.3. Boroo deposit

The Boroo deposit is the largest gold deposit in the Dzuunmod area and has been mined as an open-pit mine with four main ore zones from 2004 to 2010 (Cluer et al., 2005; Khishgee and Akasaka, 2015). The NE-trending Boroo thrust fault, which is the part of the Yeroogol fault system, develops (Fig. 4d) and has been considered to control the gold mineralization in the deposit (Cluer et al., 2005). The fault separates the Haraa Group and the Boroogol Complex. The sulfidized granite of Boroogol Complex in the Boroo deposit undergoes great siliceous and carbonatic alterations and mainly consists of plagioclase, K-feldspar and quartz (Fig. 5i). A few sericite grains develop along the fractures within the rock. The altered sandstone and silicified granite contains the gold and sulfide grains as a disseminated form, stockwork and quartz veins. The alteration assemblages are very similar to those of the Gatsuurt deposit and the most pervasive alteration represents a quartz-sericite-carbonate assemblage. Pyrite and arsenopyrite are the most abundant sulfide minerals with minor amount of sphalerite, galena and chalcopyrite (Fig. 6h). Native gold grains are observed in the quartz veins and as a disseminated in the host rocks.

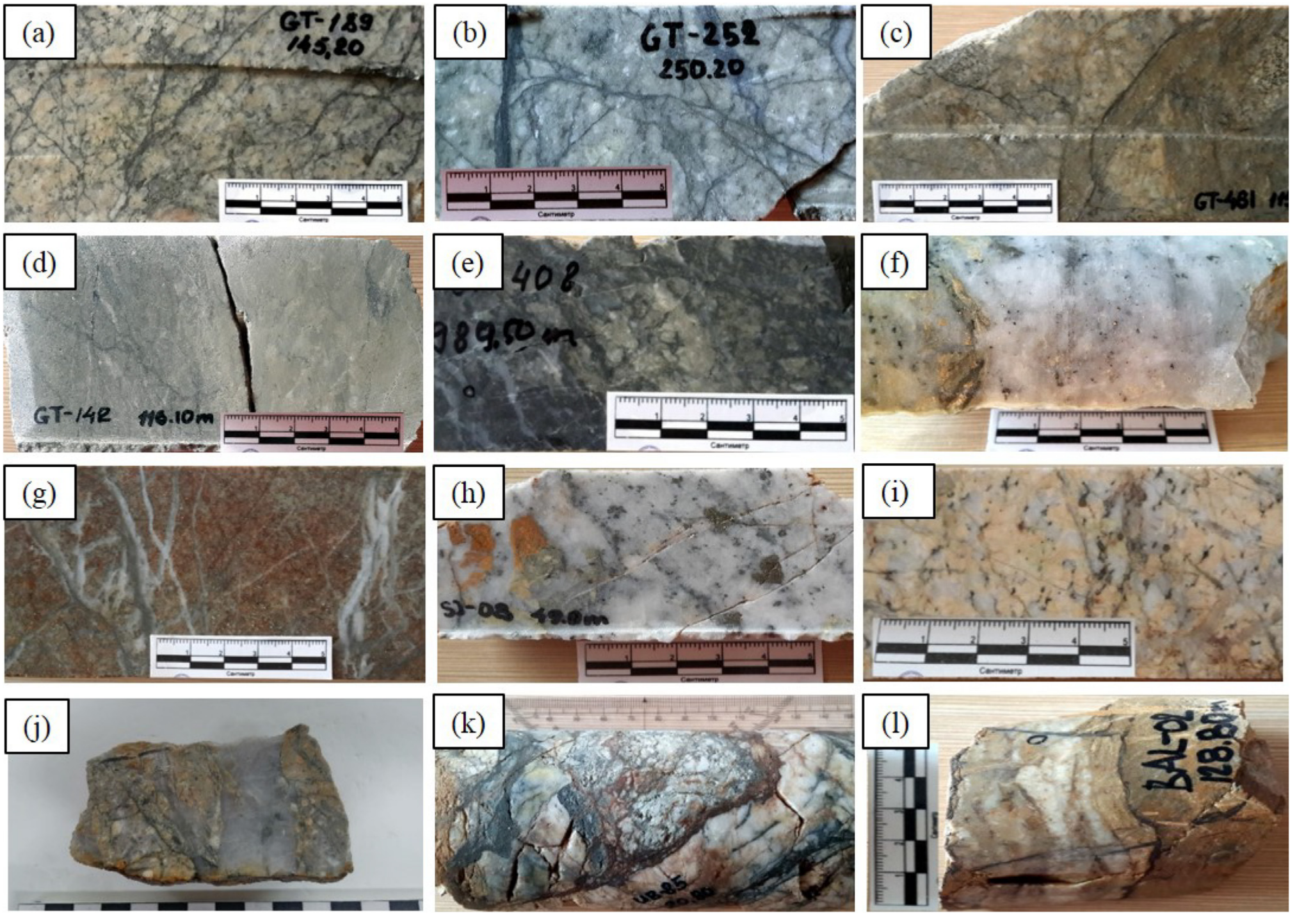

Fig. 5. Photographs of drill cores and hand specimens from Gatsuurt deposit (from a to f), Sujigtei deposit (g & h), Boroo deposit (i), Ereen deposit (j), Ulaanbulag deposit (k) and Balj occurrence (l) in the Dzuunmod area. (a) sulfidized granite in the Central zone, (b) rhyolite dike with quartz veins in the Main zone, (c) diorite influenced by siliceous alteration, (d) sulfidized sandstone, (e) silicified granite & (f) quartz vein in granite, (g) granite effected by sericitic and carbonatic alteration with quartz veins, (h) quartz veins, (i) silicified granite, (j) altered rhyolite with quartz vein, (k) quartz veinlet with sulfide grain in granite, (l) quartz veins in sandstone.

4.4. Other deposits and occurrences

The Ereen deposit is located in the central part of the Dzuunmod subvolcanic Complex and about 3.4 km west away from the Gatsuurt deposit (Fig. 3). It was discovered in early 20th century and two quartz veins with NE-trending has been explored by ten trenches. The main host rocks are volcanic rocks such as altered rhyolite (Fig. 5j) and the gold-bearing veins are controlled by faults. The rhyolite porphyry of Dzuunmod subvolcanic Complex in Ereen deposit is composed of plagioclase, K-feldspar and quartz phenocryst (25–30%) with groundmass (70–75%) affected by sericitic and siliceous alteration processes (Fig. 5j). The major alteration types of the Ereen deposit are very similar to those of the Gatsuurt deposit, which are sericitic, siliceous and potassic alteration. The sericitic alteration occurs near the quartz veins and ore minerals such as pyrite, arsenopyrite, gold, galena, sphalerite and chalcopyrite exist within quartz veins. The gold grains are present as both native form and invisible gold in the sulfide minerals.

The Ulaanbulag deposit is about 19 km away from the Gatsuurt deposit (Fig. 3) and was discovered in 2003 as a small deposit with low grade. The host rocks are the Haraa Group and the Boroogol Complex intruding the Haraa Group. The biotite granite in Ulaanbulag deposit consists of plagioclase, K-feldspar, quartz and biotite where quartz veins develop (Fig. 5k). Diorite (quartz, plagioclase and biotite) and granodiorite (quartz, plagioclase and K-feldspar) also occur in the Ulaanbulag deposit. The Ulaanbulag thrust fault is major structural feature controlling the gold mineralization. An alteration assemblage of quartz, sericite and pyrite occurs and the mineralization types consist of the quartz veins (Fig. 5k) and the disseminated/stockwork. Pyrite, arsenopyrite, iron oxides and visible gold are present with minor amount of galena, chalcopyrite and sphalerite.

The Balj occurrence is located 4.5 km away from the Gatsuurt deposit (Fig. 3). It was explored and mined from 2010 to 2012 as both open pit and under-mining style, but could not be further mined due to low grade and tonnage of gold. The host rocks are the *meta*-sedimentary rocks (Haraa Group) and the Boroogol Complex. The NE-trending fault (N20E/40SE) in the Balj occurrence is considered to control the mineralization processes in this area. The auriferous quartz veins occur in the sandstone (Fig. 5l). The alteration type and ore mineralogy is very similar with the Gatsuurt deposit, which is pervasive quartz and sericite assemblage with pyrite and arsenopyrite as major sulfide minerals.

The Biluut occurrence is located near the Gatsuurt deposit (Fig. 3) and hosted by the Dzuunmod subvolcanic Complex. The mineralization occurs along the NE-trending fault (N30E/40SE), representing a branch of the Sujigtei fault zone. Rhyolite porphyry in the Biluut occurrence is composed of plagioclase, K-feldspar and quartz phenocryst (10–15%) with groundmass (85–90%). Plagioclase is slightly altered into sericite occurring along the fractures. The gold mineralization type is quartz vein controlled by fault and major sulfide minerals are pyrite and arsenopyrite within the quartz vein.

The Khargana deposit is situated in the southern part of the Dzuunmod subvolcanic Complex and 15 km away from the Gatsuurt deposit (Fig. 3). It has been developed as a small underground mine.

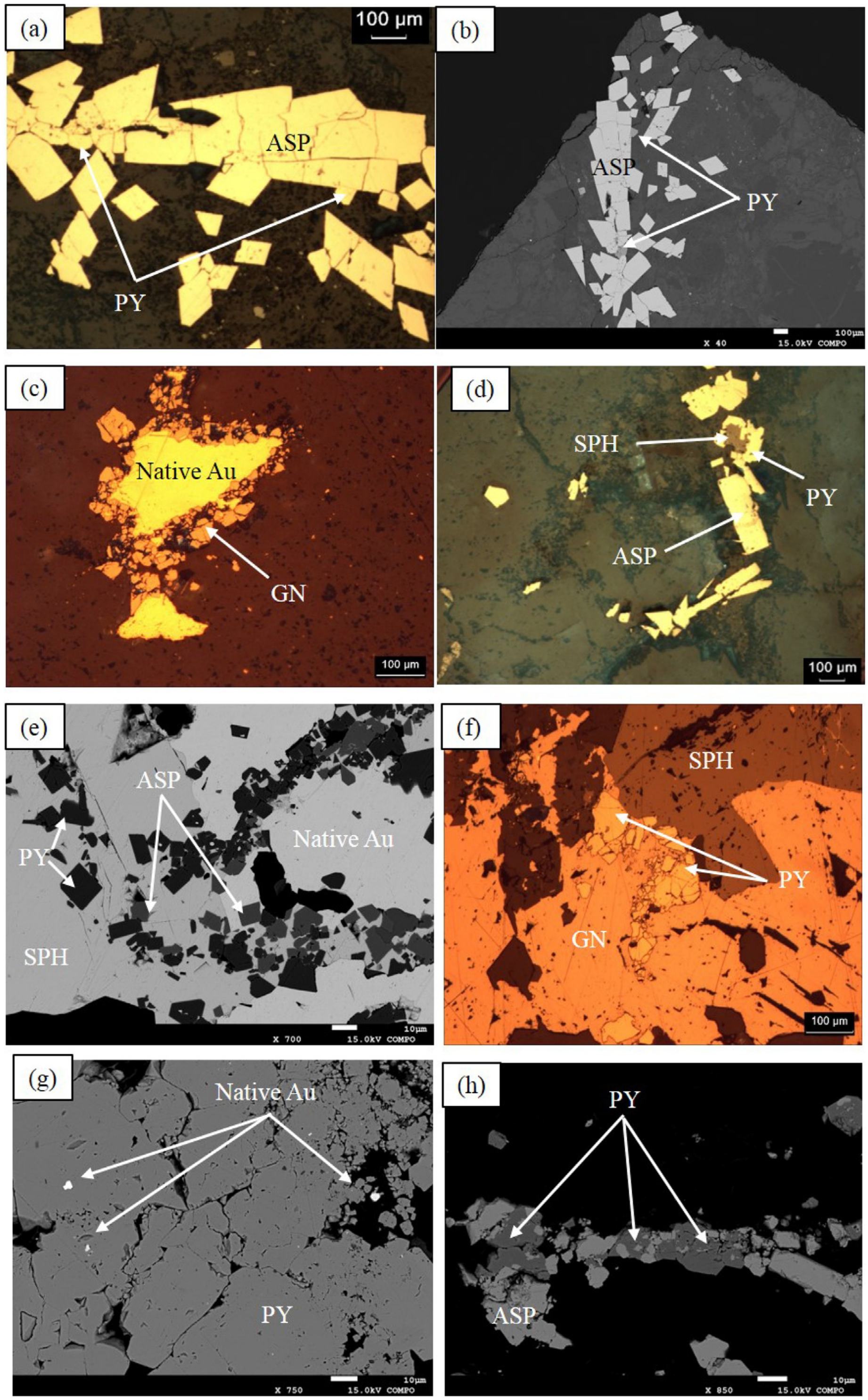

Fig. 6. Representative reflected-light photomicrographs and BSE images of sulfide minerals and native gold in the Dzuunmod area. (a) & (b) pyrite and arsenopyrite in disseminated and stockwork type, (c) native gold with galena, (d) pyrite and arsenopyrite with sphalerite & (e) native gold, pyrite, arsenopyrite and sphalerite in quartz vein type in Gatsuurt deposit, (f) pyrite, galena and sphalerite & (g) native gold grain within pyrite grain in Sujigtei deposit, (h) pyrite and arsenopyrite in Boroo deposit. PY: pyrite, ASP: arsenopyrite, SPH: sphalerite, GN: galena.

The main host rock is rhyolite and the gold mineralization is composed of the disseminated/stockwork and the quartz vein type with an assemblage of quartz, sericite and K-feldspar. The major sulfide minerals are pyrite and arsenopyrite with few Cu-bearing sulfide minerals and galena. The quartz veins are parallel to the NE-trending Sujigtei fault with steep southeast dip.

4.5. Paragenetic sequences of ore minerals

Gold deposits in the Dzuunmod area represent similar alteration assemblages and ore mineralogy usually controlled by NE-trending fault such as Sujigtei fault. Previous studies reported the mineralogical and petrological observation of the Gatsuurt and the Boroo deposit, which are the largest deposits in the study area (Khishgee et al., 2014;

Khishgee and Akasaka, 2015). First two types of mineralization occur in the Boroo deposit without silicified zone. They divided each mineralization type into four stages in disseminated and stockwork type, five stages in quartz vein type and two stages in silicified ore type.

Quartz is major gangue mineral pervasively developed in all deposits. Major ore minerals, pyrite and arsenopyrite, occur in all mineralization types, but are concentrated in early stages of each types. Both minerals are more abundant in disseminated and stockwork ores, and silicified ores than quartz vein ores. Interestingly, auriferous pyrite and arsenopyrite postdates the non-auriferous ones in the Gatsuurt deposit and Boroo deposit. Native gold mineralization occurs after the major sulfide mineralization stages. Other minor sulfides including galena, sphalerite, chalcopyrite, tetrahedrite, tennantite and bournonite vary depending on the ore types and deposits. In the Gatsuurt deposit, these minerals occur after the precipitation of major sulfide minerals in the disseminated and stockwork ore types, whereas they exist with major ore minerals in the quartz vein ores. In contrast, other minor sulfide minerals postdate the occurrence of major ore minerals in both ore types in the Boroo deposit. Therefore, it is considered that there are slightly different ore mineral assemblages in sulfidized and quartz vein ore types. The paragenetic sequences of ore minerals and quartz are summarized in Fig. 7.

5. Trace element geochemistry

Pyrite and arsenopyrite are the most abundant sulfide minerals in the Dzuunmod area. Iron (Fe) content of pyrite grains ($n = 137$) ranges from 43.64 wt% to 46.59 wt% with an average of 45.56 wt% in the study area (Supplementary Table 1). S content of pyrite grains in these deposits ranges from 49.39 wt% to 53.80 wt% with an average of 52.25 wt% (Supplementary Table 1).

Variation of sulfur (S) content of pyrite is closely related to As content in pyrite grains. Pyrite grains in the Sujigtei deposit show distinctly lower range and average value of As content ranging from 0.02 wt% to 0.52 wt% (avg. 0.20 wt%), whereas S content ranges from 52.58 wt% to 53.80 wt% with an average of 53.17 wt%. In contrast, higher As and lower S content are observed in the Gatsuurt deposit (As: 0.09–5.87 wt% (avg. 1.68 wt%), S: 49.39–53.32 wt% (avg. 51.86 wt%)) and in the Boroo deposit (As: 0.73–2.70 wt% (avg. 1.35 wt%), S: 51.22–52.28 wt% (avg. 51.77 wt%)). This relationship between S content and As content indicates a substitution of As for S in pyrite grains (e.g., Blanchard et al., 2007).

Au and As content of the Au-bearing pyrite and arsenopyrite grains can be used to predict not only the saturation state, but the chemical state of Au incorporated into them (Reich et al., 2005; Su et al., 2008; Sung et al., 2009; Khishgee and Akasaka, 2015; Yuan et al., 2018). Reich et al. (2005) suggested an empirical solubility limit of Au in Au-bearing pyrite and arsenopyrite defined as a line with an equation of

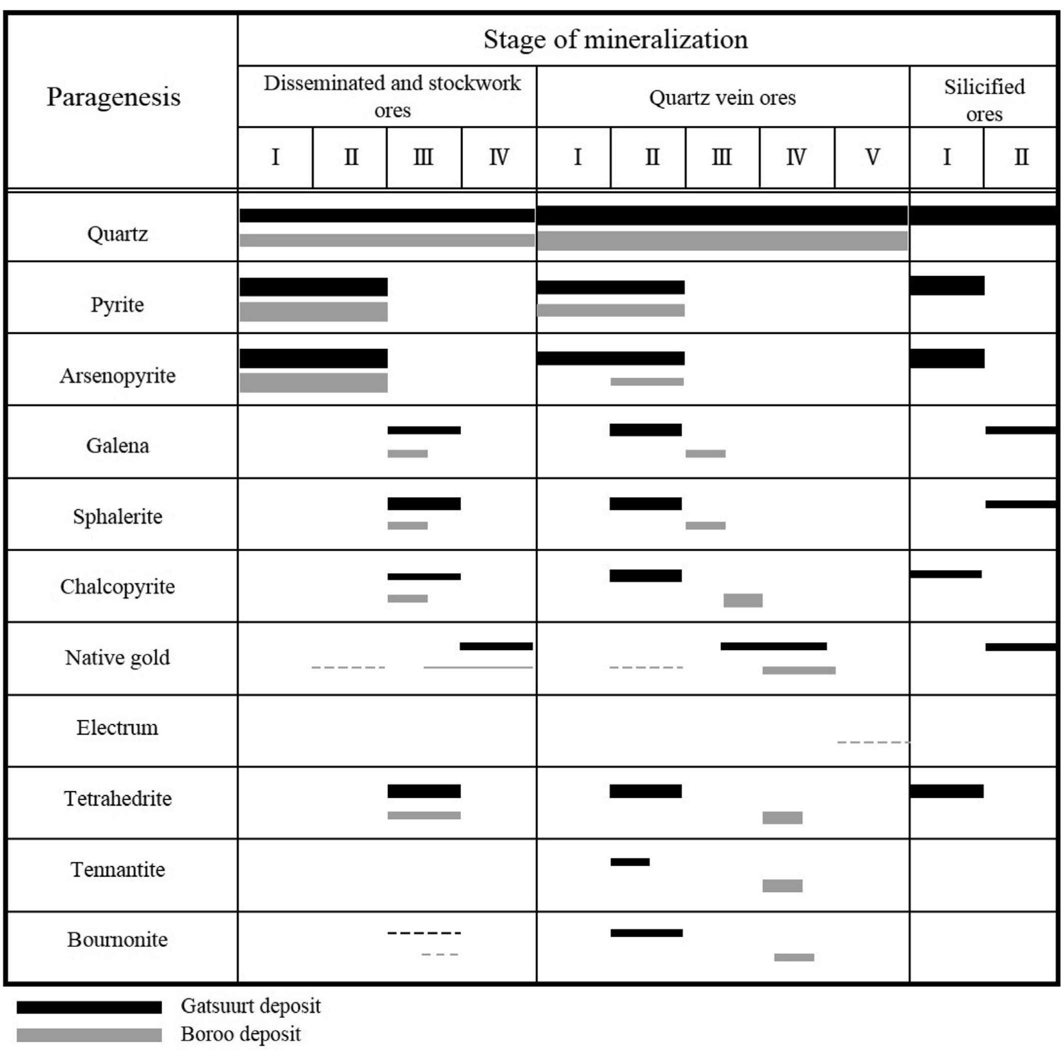

Fig. 7. Mineral paragenetic sequences of the Gatsuurt deposit and Boroo deposit modified from Khishgee et al. (2014) and Khishgee and Akasaka (2015).

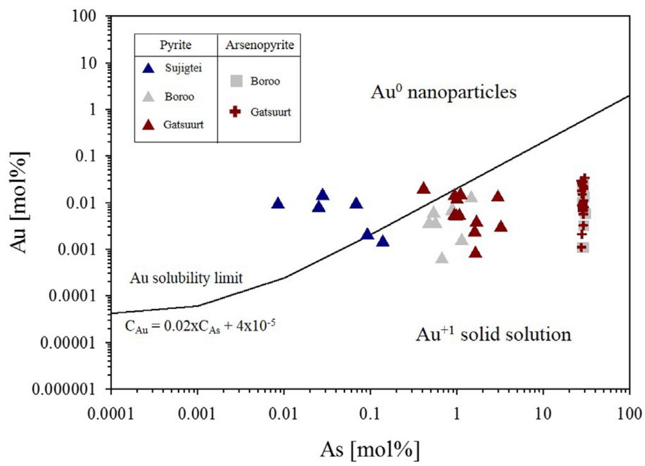

Fig. 8. Au-As diagram with Au solubility line defined by Reich et al. (2005) and plots of pyrite and arsenopyrite from Gatsuurt, Boroo and Sujigtei deposit.

$C_{Au} = 0.02xC_{As} + 4x10^{-5}$ where C_{Au} and C_{As} indicates the mole % of Au and As, respectively. As shown in Fig. 8, plots above the line indicates that gold occurs mainly as Au^0 nanoparticles whereas Au exists as Au^{+1} ion in solid solution in the plots below the line. In this study, all measured arsenopyrite grains and most pyrite grains except one grain from the Gatsuurt and Boroo deposit are plotted below the solubility line of Au while most plots of pyrite grains from the Sujigtei deposit are present above the line (Fig. 8). This suggests that gold exists mainly as Au^{+1} of solid solution in pyrite and arsenopyrite of the Gatsuurt and Boroo deposit. In contrast, gold was present as nanoparticles in pyrite grains at the Sujigtei deposit.

Whereas the Gatsuurt and Boroo deposit where pyrite and arsenopyrite are most abundant sulfide minerals, few arsenopyrite is observed in the Sujigtei deposit. Considering the lower As content of pyrite grains in the Sujigtei deposit (Supplementary Table 1), this suggests the deficiency of As in hydrothermal fluid and/or unfavorable condition of As precipitation. When As substitutes S in pyrite structure during As pyrite formation, more As can enter into pyrite grain under an anoxic condition of its precipitation (Mango and Ryan, 2015) and Au positively related to As is more easily able to be incorporated into pyrite or arsenopyrite (Yuan et al., 2018). This indicates that if As is not deficient, the hydrothermal fluid of the Sujigtei deposit was under more oxic condition than the other deposit, restraining the precipitation of Au-bearing minerals.

This higher oxidation state of ore-forming fluid is consistent with the lack of disseminated and stockwork ore type in the Sujigtei deposit compared to two other deposits. Only a quartz vein type developed in the Sujigtei deposit, whereas both disseminated and stockwork type and quartz vein type formed in the Gatsuurt and Boroo deposit (Fig. 7). Because the disseminated and stockwork mineralization process accompanied with Fe-sulfidation leads to the reduction of ore-forming fluid (Palin and Xu, 2000), the absence of this ore type in the Sujigtei deposit indicates a different oxidation state of ore-forming fluid. Therefore, the Sujigtei deposit underwent the single-type ore-forming process restricted to quartz vein type and the different oxidation state of ore-forming fluid led to lower As and Au contents. These results indicate that the conditions of hydrothermal fluid were variable and, in turn, this difference led to completely contrasting result of gold mineralization between the Gatsuurt and Boroo deposit where mining has been available, and Sujigtei deposit with low grade and tonnage.

Co and Ni content of pyrite grains in the study area ranges from 0.01 wt% to 0.68 wt% with an average of 0.05 wt% and from 0.01 wt% to 0.08 wt% with an average of 0.02 wt% (Supplementary Table 1). The Co content is generally higher than the Ni content showing larger variation and average value. Little difference of average value and total variation of both Co and Ni contents is observed among deposits, indicating that there is no spatial variation of these elements in the study area.

Both Co and Ni content in pyrite grains have been used to distinguish the sources of hydrothermal fluid because both elements are derived from mantle, but show different behavior (e.g., Li et al., 2014; Niu et al., 2016; Yuan et al., 2018). Ni represents more compatible behavior rather than Co, indicating that Ni is preferentially moved into solid phase during early stage of magma and hydrothermal fluid evolution. As an empirical parameter, the Co/Ni ratio greater than one in pyrite is considered to indicate the influence from hydrothermal fluid on the deposit (Clark et al., 2004; Li et al., 2014; Niu et al., 2016; Yuan et al., 2018).

Calculated Co/Ni ratio of pyrite grains (*n = 63)* has an average value of 4.49 from 0.44 to 45.2. Considering the higher content of Co than Ni, most Co/Ni ratios greater than one suggests that the hydrothermal fluid in the Dzuunmod area was greatly influenced by fluid-host rock interaction during mineralization processes. More incompatible behavior of Mo than Co and Ni causes an enrichment in differentiated igneous rocks. This indicates that the Mo/Ni ratios of pyrite grains are able to infer the relative strength of (ultra)-mafic rock over felsic rocks such as granite in the source region (Koglin et al., 2010; Yuan et al., 2018). The Mo content of pyrite grains in the study area shows one order greater value than Co and Ni, which is approximately 0.45 wt% as an average value in each deposit (Supplementary Table 1). This makes the extremely large (one order higher) Mo/Ni ratios of pyrite grains in the Dzuunmod area from 5.51 wt% to 479 wt% (avg. 34.7 wt%), suggesting a felsic rock provenance for metal sources. The dominance of felsic provenance also seems to be consistent with the major host rocks (granite, diorite and rhyolite) in the Dzuunmod area.

Koglin et al. (2010) suggested that both high Co/Ni and Mo/Ni ratio are characteristics of post-sedimentary or hydrothermal origin of pyrite and the composition of hydrothermal fluid may be intensely affected by fluid-rock interaction. The measured elemental ratios of pyrite grains are not able to provide a direct information about the original hydrothermal fluid before fluid-host rock interaction. This implies that it is unclear whether the original hydrothermal fluid was preserved during mineralization processes in the Dzuunmod area. Therefore, the signals of post-sedimentary or hydrothermal origination are inherited either from original fluid or by host rock during mineralization processes in the Dzuunmod area.

6. Stable isotope systematics

6.1. Sulfur isotope data

Pyrite and arsenopyrite are the most abundant sulfide minerals with minor amount of chalcopyrite, galena and sphalerite in the Dzuunmod area. Even though changes of several physico-chemical factors such as temperature, pressure, oxygen fugacity and pH are able to influence the S isotope composition of both sulfide minerals and ore-forming fluid, the $\delta^{34}S$ value of sulfide minerals is generally corresponding to that of total sulfur species of hydrothermal fluid where they precipitated under a reduced fluid system such as the mineral association of pyrite-arsenopyrite-pyrrhotite (Ohmoto and Rye, 1979; Taylor, 1987; Seal, 2006; Hoefs, 2018). It means that the sulfide minerals seem to be precipitated from a reduce fluid as a simple mineral assemblage and their $\delta^{34}S$ value reflects the $\delta^{34}S$ of fluid.

The sulfide minerals in the Dzuunmod area represent a wide variation of the $\delta^{34}S$ values from −2.6‰ to 17.2‰ with an average of 2.1‰ (Table 2). The arsenopyrite has a larger variation of $\delta^{34}S$ values from −2.6‰ to 17.2‰, whereas the $\delta^{34}S$ values of pyrite range from −0.7‰ to 9.3‰ (Fig. 9). However, the average $\delta^{34}S$ value of pyrite and arsenopyrite is 2.3‰ and 1.9‰ respectively, which is very similar to the $\delta^{34}S$ value of total sulfide as well as themselves. The paragenetic sequences of the ore minerals also show that pyrite and arsenopyrite

Table 2
Sulfur isotope compositions of pyrite and arsenopyrite in the Dzuunmod area.

Deposit	Sample	Mineral*	Mineralization type	Host rock	$\delta^{34}S$		
					I	II	mean
Gatsuurt	GT-189_145.20 m	py	disseminated sulfide	sulfidized granite	−0.2	0.2	0.0
	GT-280_104.50 m	py		sulfidized rhyolite with porphyry texture	2.6	3.1	2.8
	GT-437_89.20 m	py		sulfidized granite with stockwork and quartz-sulfide veins	−0.7		−0.7
	GT-461_115.80 m	py		altered diorite with quartz-sulfide veins	2.6	2.8	2.7
	GT-461_130.30 m	py		sulfidized granite with stockwork and quartz-sulfide veins	1.1		1.1
	GT-490_170.80 m	asp		diorite with quartz-carbonate veins	−2.2		−2.2
	GT-95_80.80 m	asp	quartz vein	altered sandstone	0.3		0.3
	GT-376_203.20 m	asp		sulfidized rhyolite porphyry	17.0	17.4	17.2
	GT-461_108.60 m	asp		quartz vein with sulfide in granite	−0.2		−0.2
	GT-221_66.40 m	py	silica	siliceous altered granite with VG	0.9		0.9
	GT-49_43.50 m	asp		silica zone with sulfide VG and breccia texture	−1.5		−1.5
	GT-189_22.45 m	py		silica zone in granite with veinlets	1.0	0.5	0.7
	GT-408_989.50 m	asp		Pervasive Quartz Silica zone	1.3		1.3
	GZ	asp		altered rhyolite	−2.6		−2.6
Sujigtei	SJ-006_165.50 m	py	quartz vein	sulfidized rhyolite with weak siliceous and sericite alteration	2.7		2.7
Ereen	ER-10/1	asp	quartz vein	quartz vein in sulfidized rhyolite porphyry	4.4	4.2	4.3
Boroo	BR-P-6	py	disseminated sulfide	sulfidized sandstone	−0.1	−0.9	−0.5
	MDD-008	py		granite with stockwork and quart veinlets	4.1	4.3	4.2
Ulaanbulag	UB-79_62.20 m	py	disseminated sulfide	quartz vein with sulfide in granite	1.7		1.7
Khargana	KH-P-1	py	quartz vein	sulfidized rhyolite porphyry	9.0	9.6	9.3
Biluut	Bi-07_109.60 m	asp	quartz vein	rhyolite porphyry to stockwork or breccia with potassic alteration	0.3		0.3
	Bi-07_113.90 m	py	disseminated sulfide	brecciated rhyolite porphyry	4.7	4.9	4.8

* The py and asp indicate pyrite and arsenopyrite, respectively.

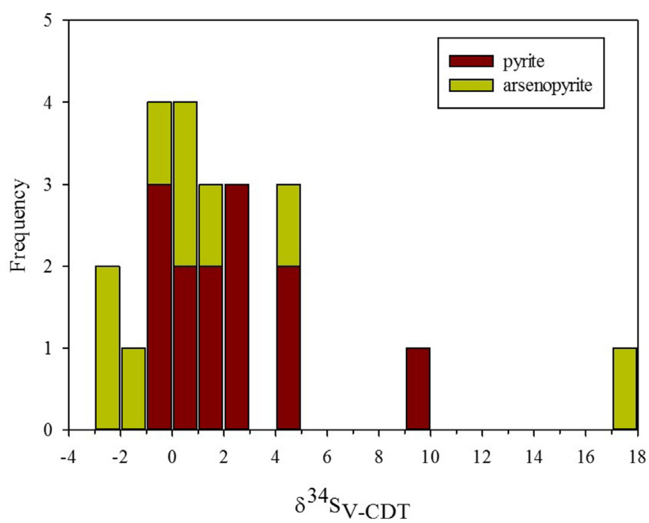

Fig. 9. Histogram of sulfur isotope composition ($\delta^{34}S$) of pyrite and arsenopyrite in the Dzuunmod area.

were precipitated in the similar stages (Fig. 7). Therefore, it is considered that they were precipitated from the hydrothermal fluids with similar $\delta^{34}S$ values and did not undergo the S isotope fractionation between them during the precipitation event.

Relatively large range of $\delta^{34}S$ values enables to exclude a possibility that a magmatic sulfur plays a dominant role of sulfur source in the Dzuunmod area. The $\delta^{34}S$ value of magmatic sulfur is close to 0‰ and sulfide minerals in the various ore deposits where the sulfur is mainly derived from the deep magma show very restricted range of the $\delta^{34}S$ values near 0‰ (e.g., Ohmoto, 1972; Taylor, 1987; Seal, 2006). This may indicate that average $\delta^{34}S$ value in the Dzuunmod area reflects the magmatic derivation of sulfur. However, only magmatic sulfur cannot explain large $\delta^{34}S$ values of sulfide minerals such as 4.8‰, 9.3‰ and 17.2‰, which are too far from the $\delta^{34}S$ value of magma. In orogenic gold deposits, the $\delta^{34}S$ values of major sulfide minerals where sulfur is derived from a deep-seated magmatic source show a relatively smaller variation (e.g., Ding et al., 2016; Ma et al., 2018; Yuan et al., 2018).

Compared to the magmatic sulfur, the $\delta^{34}S$ values of sedimentary and metamorphic rocks show much wider variation approximately from −40‰ to 50‰ and from −20‰ to 20‰, respectively (Hoefs, 2018 and references therein).

The heterogeneous S isotope composition of sulfur sources attributes to the observed large variation of $\delta^{34}S$ values rather than the changes of S isotope composition of fluid during fluid migration or sulfide deposition. This means that the possible sulfur sources have large range of $\delta^{34}S$ values in the study area. Several studies suggested that syngenetic and diagenetic pyrite produced by both bacterial and thermochemical seawater sulfate reduction processes could be possible sulfur sources in the sediment-hosted orogenic gold deposit (e.g., Chang et al., 2008; Goldfarb and Groves, 2015; Zhang et al., 2018). Because both biotic and abiotic sulfate reduction can trigger a large S isotope fractionation up to 50‰, resulting in the depletion of the heavier isotope (^{34}S) in a reduced sulfur species (Krouse and Mayer, 2000; Seal, 2006; Hoefs, 2018 and references therein), the syngenetic and diagenetic pyrite in the marine sediment have a wide range of $\delta^{34}S$ values. During the metamorphic event of the pyrite-bearing sedimentary rocks, the sulfur seems to be put into the metamorphic fluid, possibly ore-forming fluid, and transported to the deposit site (Goldfarb, 1997; Goldfarb et al., 2005; Goldfarb and Groves, 2015)

The mixing of multiple sulfur sources or S isotope fractionation of sulfur species in ore-forming fluids driven by progressive oxidation of them can influence the $\delta^{34}S$ values of minerals in the orogenic gold deposit (Chang et al., 2008; Xu et al., 2017; LaFlamme et al., 2018a; Ma et al., 2018), making it more difficult to constrain the sulfur sources. For example, Xu et al. (2017) and Zhang et al. (2018) proposed a slightly different sulfur sources in the orogenic gold deposit in Jiangnan orogeny region, south China. The former suggested a mixing of metamorphosed sulfur source and magma-derived sulfur, whereas the latter insisted of a single metamorphic sulfur source affected by S isotope fractionation processes during sulfide deposition. This implies that the $\delta^{34}S$ signal of original sulfur sources can be altered during migration of hydrothermal fluid and/or mineralization event.

Many studies interpreted the decreasing trend of $\delta^{34}S$ values of sulfide minerals depending on the precipitation order as an effect of the isotopic fractionation by fluid oxidation during mineralization process such as sulfidation and carbonatization (e.g., Uemoto et al., 2002;

Evans et al., 2006; Neumayr et al., 2008; Hodkiewicz et al., 2009; Ward et al., 2017; LaFlamme et al., 2018b; Ma et al., 2018). Especially, fluid-rock interaction such as carbonatization and sulfidation has been suggested as a major gold precipitation process in orogenic gold deposits, causing the oxidation of ore-forming fluids (e.g., Phillips and Groves, 1983; Phillips et al., 1986; Palin and Xu, 2000; Ridley and Diamond, 2000; Evans et al., 2006; Neumayr et al., 2008). Both reactions include the formation of Fe-Ca-Mg carbonates and iron-bearing sulfides respectively within the host rocks, causing the oxidation of ore-forming fluids. The variation of fluid oxidation state and subsequent decrease of activity of the reduced sulfur species triggers the decrease of gold solubility by destabilizing the gold bisulfide complexes, leading to the gold precipitation. Geological evidences of the Dzuunmod area represent the presence of widespread wall-rock sulfidation and, to a lesser extent, carbonatization reactions during precipitation events. The occurrence of sulfidation and carbonatization, therefore, indicates that these reactions played a significant role in gold precipitation in the study area.

The $\delta^{34}S$ values measured in this study suggest that the sulfidation, rather than carbonatization, contributed more importantly to the formation of gold deposits in the study area. According to modelling result, both reactions resulted in the reduction of ore-forming fluid and decrease of activity of the reduced sulfur species, necessary for the decrease of gold solubility, but completely different evolutionary pathways of S isotope composition (Palin and Xu, 2000). The $\delta^{34}S$ value of ore-forming fluid shifts insignificantly during sulfidation reaction because it stays within pyrite-pyrrhotite stability field (Palin and Xu, 2000 and references therein). In contrast, substantial variation of $\delta^{34}S$ value accompanied with fluid oxidation and decrease of activity of reduced sulfur species within fluid during carbonatization reaction occurs owing to the change of oxidized (HSO_4^-) and reduced (H_2S) sulfur species (Phillips and Groves, 1983; McCuaig and Kerrich, 1998; Palin and Xu, 2000; Evans et al., 2006). The fluid oxidation brings about the increase of HSO_4^- in fluid, leading to the rise of proportion of HSO_4^- to H_2S. Because the heavier S isotope (^{34}S) tends to be enriched in HSO_4^- rather than H_2S in the hydrothermal fluid, the H_2S species remained in the fluid and the products of sulfides become lighter (Ohmoto and Rye, 1979). The negative mean and range of $\delta^{34}S$ values of sulfide minerals in orogenic gold deposits is a diagnostic of the presence of carbonatization reaction (e.g., Palin and Xu, 2000; Hodkiewicz et al., 2009). Therefore, relatively positive $\delta^{34}S$ values measured in this study cannot be explained by carbonatization reactions.

Even though some sulfide samples in this study show negative $\delta^{34}S$ values, most $\delta^{34}S$ values and mean value are positive (Table 2). This indicates that the sulfidation is a predominant fluid-host rock interaction for gold precipitation in the Dzuunmod area. In addition, the measured $\delta^{34}S$ values are consistent with the geological observation, which is the occurrence of the widespread disseminated sulfides. This implies that the $\delta^{34}S$ values of sulfur species in the ore-forming fluid in the study area might be preserved during gold precipitation processes. Even though the influence of carbonatization cannot be completely discounted because of the existence of carbonatization alteration, the $\delta^{34}S$ values enable to exclude the carbonatization and phase separation as a major mechanism for gold precipitation.

6.2. Oxygen isotope data

The measured $\delta^{18}O_{quartz}$ values of the Dzuunmod area vary from 14.7‰ to 17.7‰ with a narrow range (3‰) indicating a homogeneous oxygen isotope composition of quartz vein samples (Table 3). When hydrothermal fluid flows along the fault or channel to mineralization site, a highly fluid-dominant condition is likely to prevent the modification of $\delta^{18}O_{fluid}$ values (Goldfarb and Groves, 2015). This means that the ore-forming fluid keeps its oxygen isotope composition along the fluid path without fluid mixing during mineralization processes usually by later influx of meteoric water. Therefore, the homogeneity of

Table 3
Oxygen isotope composition of quartz samples and calculated $\delta^{18}O$ values of ore-forming fluid in the Dzuunmod area.

Deposit	Sample	Mineralization type	$\delta^{18}O_{V\text{-}SMOW}$ (‰)	
			Quartz	Fluid*
Gatsuurt	GT-372_99.60 m	Quartz vein	16.5	8.2
	GT-172_357.80 m	Quartz vein	15.0	6.7
	GT-93_38.40 m	Quartz vein	15.2	6.8
	GT-462_126.0 m	Quartz vein	16.1	7.7
	GT-408_989.30 m	silica	14.7	6.3
	GT-94_96.40 m	silica	15.4	7.0
	GT-339_138.40 m	silica	16.7	8.3
Sujigtei	SJ-08_49.0 m	Quartz vein	15.5	7.2
Ereen	ER-7-q	Quartz vein	16.0	7.7
Boroo	BDD-105_40.60 m	Quartz vein	16.2	7.9
	KH-BOR-4_136.0 m	Quartz vein	16.2	7.9
Ulaanbulag	UB-79_60.85 m	Quartz vein	17.0	8.6
Biluut	BI-07_114.30 m	Quartz vein	17.4	9.1
Balj	BAL-02_136.75 m	Disseminated	17.7	9.3

* The temperature of the ore-forming fluid is 275 °C estimated from arsenopyrite geothermometry.

$\delta^{18}O_{quartz}$ values in the Dzuunmod area is likely to imply the absence of influx of meteoric water during ore-forming processes.

The $\delta^{18}O_{quartz}$ values can be converted into the oxygen isotope composition of hydrothermal fluid ($\delta^{18}O_{water}$) where quartz grains precipitate on the assumption that they are in equilibrium state. The $\delta^{18}O_{water}$ is calculated using an equation under the temperature condition between 200 and 500 °C as follows:

$$1000\ln\alpha^{quartz}_{water} = \delta^{18}O_{quartz} - \delta^{18}O_{water} = \frac{3.38 \times 10^6}{T^2} - 2.90$$

where α is the isotopic fractionation factor between quartz and hydrothermal fluid and T is the absolute temperature (K) (Friedman and O'Neil, 1977). This indicates that the higher mineralization temperature is, the smaller the isotopic fractionation factor becomes.

For the calculation of $\delta^{18}O_{water}$ values, the mineralization temperatures of the ore-forming fluids were obtained from the arsenopyrite geothermometry estimating the T-fS_2 conditions of mineralization with atomic percentage of As in arsenopyrite (at. % As) in the Fe-As-S system where arsenopyrite and arsenic pyrite coexist (Clark, 1960; Barton, 1969; Kretschmar and Scott, 1976). The measured As contents of arsenopyrite have an average of 29.2 at. % As (from 28.0 to 30.9 at. % As) in the study area (Supplementary Table 2). As shown in Fig. 10, these values are corresponding to the estimated mineralization temperature of 275 ± 15 °C, which is included in the range of the homogenization temperatures for fluid inclusions in quartz of the Gatsuurt deposit from 194 to 355 °C reported by Khishgee et al. (2014). However, this previously reported range of homogenization temperatures seems to be unlikely to reflect the variation of mineralization temperatures. Goldfarb and Groves (2015) argued that when the measured $\delta^{18}O_{quartz}$ values are clustered within a few ‰ the mineralization temperature is also consistent and variable homogenization temperature results are attributed to the measurement of post-ore or modified inclusions.

Based on the measured $\delta^{18}O_{quartz}$ values and the temperature data obtained from the arsenopyrite geothermometry, the calculated $\delta^{18}O_{water}$ values vary from 6.3 to 9.3‰ (Table 3). These ranges are consistent with those of orogenic gold deposits, which is from 5‰ to 15‰, where hydrothermal fluids seem to be derived from metamorphic sources (Fig. 11) (Taylor, 1987; McCuaig and Kerrich, 1998; Goldfarb et al., 2005; Goldfarb and Groves, 2015; Zhang et al., 2018). The $\delta^{18}O$ values of metamorphic fluid show a wide and higher variation from 3‰ to 20‰, whereas primary magmatic fluid has a restricted $\delta^{18}O$ values from 5.5‰ to 9.5‰ (Sheppard, 1986). A meteoric water has generally negative $\delta^{18}O$ value satisfying the Meteoric Water Line, meaning that the input of the meteoric water shifts $\delta^{18}O$ value of hydrothermal fluid

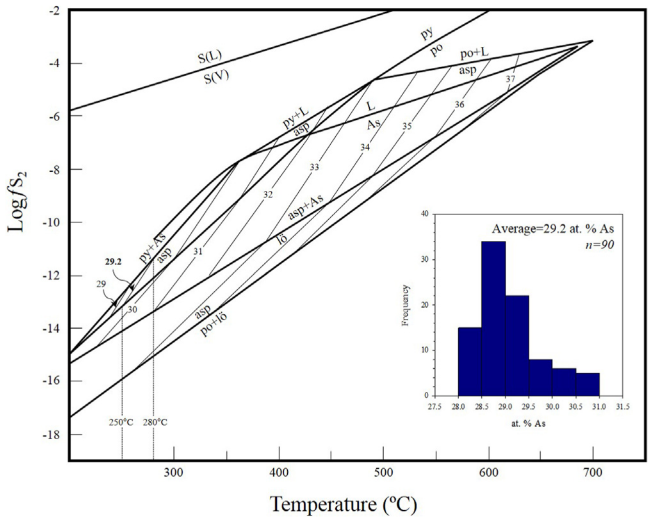

Fig. 10. Temperature – logfS_2 diagram presenting arsenopyrite and pyrite stability field with at. % As in the Fe-As-S system (after Kretschmar and Scott, 1976). The average As content of arsenopyrite in the Dzuunmod area (29.2 at.% As) is plotted in the diagram. The EPMA data of As contents in each arsenopyrite grain are present in the Supplementary Table 1. Asp: arsenopyrite, Py: pyrite, Lö: Loellingite, Po: Pyrrhotite, As: arsenic, L: sulfur-arsenic liquid.

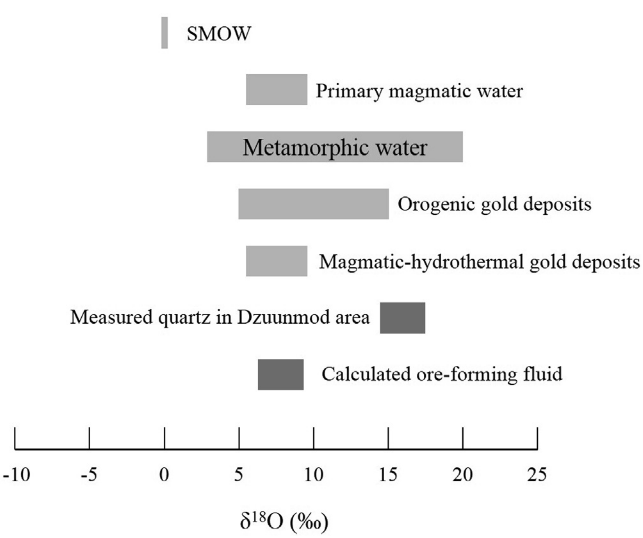

Fig. 11. $\delta^{18}O$ values of several geologically important fluid sources (Sheppard, 1986), typical orogenic and magmatic-hydrothermal gold deposits (Taylor, 1987; McCuaig and Kerrich, 1998; Goldfarb et al., 2005; Goldfarb and Groves, 2015; Ding et al., 2016; Zhang et al., 2018) and calculated ore-forming fluids from measured $\delta^{18}O$ of quartz in the Dzuunmod area.

into lower range.

The calculated $\delta^{18}O_{water}$ values overlap with those of primary magmatic water as well as metamorphic fluid, implying that the magmatic water cannot be ruled out as the ore-forming fluid sources (Fig. 11). However, the ages of host rocks are much older than mineralization ages in the Dzuunmod area, indicating that there is absence of direct genetic relationship between the formation of host rocks and mineralization events. This implies that it is unlikely that the ore-forming fluid was derived from a minor contribution of magmatic water in the study area. Considering that meteoric water will not reach the crustal depth where most orogenic gold deposits formed (Goldfarb and Groves, 2015), it is most likely that the ore-forming fluid in the Dzuunmod area was derived from metamorphic sources, consistent with their $\delta^{18}O$ values (Fig. 11).

7. Implications for ore genesis and sources

Ore-mineral assemblages, paragenetic sequences, trace element compositions and stable isotope results in this study suggest the possible gold mineralization processes in the Dzuunmod area. First, the input of hydrothermal fluid without gold altered the host rocks causing the sulfidation of iron oxides or silicates within host rocks. The precipitation of non-auriferous major sulfides occurred during this period by fluid-host rock interactions or physicochemical variations of hydrothermal fluid (Groves and Foster, 1991; Seward, 1993; Goldfarb et al., 2001; Su et al., 2008; Phillips and Powell, 2010). Second, the influx of the auriferous hydrothermal fluid where gold is mainly transported by Au^{+1} ions with bisulfide complex resulted in the sulfidation of the host rocks. Su et al. (2008) suggested that this processes reduce the activity of the sulfur species (as H_2S or HS^-) in the hydrothermal fluids, building a favorable condition for the incorporation of Au from solid solution to pyrite and arsenopyrite grains to form invisible gold, being undersaturated with respect to native gold (Simon et al., 1999; Reich et al., 2005). Then, when the released H_2S-poor fluid meets the fresh Au-bearing and H_2S-rich fluid, the saturation of native gold by the reduction of H_2S activity brings about the destabilization of Au-bisulfide complexes and lead to the precipitation of native gold grain (e.g., Seward, 1993).

This gold mineralization process suggests the multiple mineralization events by fluid-host rock interactions in the Dzuunmod area. The earlier precipitation of major sulfide minerals than native gold, which is subsequently separated into non-auriferous and invisible Au-bearing pyrite and arsenopyrite. This implies that the host rocks may influence not only the mineralization processes including paragenetic sequences and the form of Au-bearing minerals, but the trace element content of sulfide minerals. Substantial difference of timing between intrusion and mineralization event suggests that mineralization is not directly associated with intrusion of the Boroogol Complex to the existing Haraa Group.

Even though the role of magmatic sulfur as one of possible sulfur sources cannot be ruled out due to the clustering of most $\delta^{34}S$ values near 0‰ with low average, the large variation of the $\delta^{34}S$ values from −2.6‰ to 17.2‰ in this study indicates the heterogeneity of S isotope composition of source materials. Because Fe-sulfidation, considered as main ore-forming mechanism in the study area, cause little S isotope fractionation during precipitation (e.g., Palin and Xu, 2000), the change of S isotope composition during migration in hydrothermal fluid and precipitation as sulfide minerals cannot be dominant mechanism to explain this variation. Therefore, the S isotope signature seems to be derived from a heterogeneous source. Because there are no outcrops of sulfate-bearing rocks in the study area (Fig. 3), a sediment-hosted pyrite with heterogeneous $\delta^{34}S$ values incorporated into metamorphic fluid during metamorphic event is more plausible for sulfur source in the Dzuunmod area.

The measured $\delta^{18}O_{quartz}$ values in the Dzuunmod area indicate the homogeneous isotope composition of hydrothermal fluid and exclude the potential modification of $\delta^{18}O_{water}$ values by the fluid mixing by later input of other fluids. This implies that the measured $\delta^{18}O_{quartz}$ values keep its original isotopic signature of ore-forming fluid. Although the calculated $\delta^{18}O_{water}$ values (from 6.3 to 9.3‰) of ore-forming fluid are not fully deviated from the area of primary magmatic water, these values are more likely to indicate a metamorphic derivation of hydrothermal fluid considering different timing of host rock formation and mineralization in Dzuunmod area. In addition, Khishgee et al. (2014) reported the CO_2-rich and halite-bearing aqueous fluid inclusions in the Gatsuurt deposit, which is consistent characteristics of fluid inclusion type occurring in ore-forming fluid of the orogenic gold deposit (Goldfarb and Groves, 2015).

8. Conclusions

Gold deposits and occurrences in the Dzuunmod area are hosted in Haraa Group, Boroogol Complex and Dzuunmod subvolcanic Complex showing similar hydrothermal alteration assemblages (sericitic, siliceous and potassic) and ore mineral assemblages (pyrite and arsenopyrite with minor amount of galena, sphalerite and chalcopyrite). The trace element composition of pyrite and arsenopyrite shows high Co/Ni and Mo/Ni ratios, indicating that these sulfides have post-sedimentary or hydrothermal origin and the ore-forming fluids were greatly affected by fluid-host rock interaction during mineralization processes. Large variation of δ^{34}S values of sulfide minerals from −2.6‰ to 17.2‰ and homogeneous δ^{18}O values of quartz from 14.7‰ to 17.7‰ indicates metamorphic derivation of sulfur and fluid even though magmatic sources cannot be ruled out.

Based on these characteristics including alteration and ore mineral assemblages, trace element data, stable isotope geochemistry, fluid inclusion and trapping temperature of fluid, and geochronological data in this and other studies (Cluer et al., 2005; Hendry et al., 2006; Goldfarb et al., 2014; Khishgee et al., 2014; Khishgee and Akasaka, 2015), the gold deposits in the Dzuunmod area has been classified into orogenic gold type where fluid and sulfur was originated from a metamorphic source. Hydrothermal fluid produced during metamorphic event was migrated to the Dzuunmod area through the NE-trending fault. Multiple gold and sulfide mineralization occurred by the sulfidation of host rocks with fluid-host rock interactions.

Acknowledgements

This research is supported by projects “NRF-2014K1A3A1A08045036” from the National Research Foundation of Korea, “20140409, PM18030” from the Ministry of Ocean and Fisheries, Korea and Korea-Mongolia joint research project “COR_03/2015” from Mongolian Science and Technology Fund. The author Y.M. Kim thanks the BK 21 program of the School of Earth and Environmental Sciences, Seoul National University.

Appendix A. Supplementary data

Supplementary data to this article can be found online at https://doi.org/10.1016/j.oregeorev.2019.103213.

References

Altanzul, C., Oyungerel, S., Jargal, L., Lee, S., Kim, Y., Khasmaral, T., 2018. Absolute age determinations of the Boroo-Dzuunmod area magmatic rocks. Explorer 59, 211–232 (in Mongolian).
Baasandolgor, L., 2003. Geologic and Geochemical Peculiarities of the Zuunmod ore District. M.Sc Thesis. Mongolian Technical University, Ulaanbaatar, in Russian.
Badarch, G., Cunningham, W.D., Windley, B.F., 2002. A new terrane subdivision for Mongolia: implications for the Phanerozoic crustal growth of Central Asia. J. Asian Earth Sci. 21 (1), 87–110.
Barton Jr, P.B., 1969. Thermochemical study of the system Fe-As-S. Geochim. Cosmochim. Acta 33 (7), 841–857.
Bierlein, F., Crowe, D., 2000. Phanerozoic orogenic lode gold deposits. *Gold in 2000*. Rev. Econ. Geol. 13, 103–139.
Blanchard, M., Alfredsson, M., Brodholt, J., Wright, K., Catlow, C.R.A., 2007. Arsenic incorporation into FeS2 pyrite and its influence on dissolution: a DFT study. Geoch. Cosmochim. Acta 71 (3), 624–630.
Bussien, D., Gombojav, N., Winkler, W., Von Quadt, A., 2011. The Mongol-Okhotsk Belt in Mongolia—an appraisal of the geodynamic development by the study of sandstone provenance and detrital zircons. Tectonophysics 510 (1–2), 132–150.
Chang, Z., Large, R.R., Maslennikov, V., 2008. Sulfur isotopes in sediment-hosted orogenic gold deposits: evidence for an early timing and a seawater sulfur source. Geology 36 (12), 971–974.
Clark, C., Grguric, B., Mumm, A.S., 2004. Genetic implications of pyrite chemistry from the palaeoproterozoic olary domain and overlying neoproterozoic adelaidean sequences, northeastern South Australia. Ore Geol. Rev. 25 (3–4), 237–257.
Clark, L.A., 1960. The Fe-As-S system–Phase relations and applications. Econ. Geol. 55 (7), 1345–1381.
Cluer, J., Kotlyar, B., Gantsetseg, O., Togtokh, D., Wood, G., Ullrich, T., 2005. Geology of the Boroo gold deposit, northern Mongolia. Seg-Iagod Guidbook Series 11, 105–117.
Dejidmaa, G., 1996. Gold metallogeny of Mongolia. Mongolian Geosci. 1, 6–29.
Deng, T., Xu, D., Chi, G., Wang, Z., Jiao, Q., Ning, J., Dong, G., Zou, F., 2017. Geology, geochronology, geochemistry and ore genesis of the Wangu gold deposit in northeastern Hunan Province, Jiangnan Orogen, South China. Ore Geol. Rev. 88, 619–637.
Ding, C., Nie, F., Jiang, S., Liu, Y., Cao, Y., 2016. Characteristics and origin of the Zhulazhaga gold deposit in Inner Mongolia, China. Ore Geol. Rev. 73, 211–221.
Donskaya, T., Gladkochub, D., Mazukabzov, A., Ivanov, A., 2013. Late Paleozoic-Mesozoic subduction-related magmatism at the southern margin of the Siberian continent and the 150 million-year history of the Mongol-Okhotsk Ocean. J. Asian Earth Sci. 62, 79–97.
Evans, K., Phillips, G., Powell, R., 2006. Rock-buffering of auriferous fluids in altered rocks associated with the Golden Mile-style mineralization, Kalgoorlie gold field, Western Australia. Econ. Geol. 101 (4), 805–817.
Friedman, I., O'Neil, J.R., 1977. Data of Geochemistry: Compilation of Stable Isotope Fractionation Factors of Geochemical Interest Vol. 440 Government Printing Office, US.
Gerel, O., Kotlyar, B., Cluer, J., Enkhtuvshin, K., Bold-Erdene, B., 1999. Geology and gold mineralization in the Khentei range. Mongolian Geosci. 14, 110–115.
Goldfarb, R., 1997. Gold deposits in metamorphic rocks of Alaska: implications for ore genesis. Econ. Geol. Monogr. 9, 151–190.
Goldfarb, R., Baker, T., Dube, B., Groves, D.I., Hart, C.J., Gosselin, P., 2005. Distribution, character and genesis of gold deposits in metamorphic terranes. Soc. Econ. Geol.
Goldfarb, R., Groves, D., Gardoll, S., 2001. Orogenic gold and geologic time: a global synthesis. Ore Geol. Rev. 18 (1–2), 1–75.
Goldfarb, R.J., Groves, D.I., 2015. Orogenic gold: common or evolving fluid and metal sources through time. Lithos 233, 2–26.
Goldfarb, R.J., Taylor, R.D., Collins, G.S., Goryachev, N.A., Orlandini, O.F., 2014. Phanerozoic continental growth and gold metallogeny of Asia. Gondwana Res. 25 (1), 48–102.
Groves, D., Foster, R., 1991. Archaean lode gold deposits. In: Gold Metallogeny and Exploration. Springer, pp. 63–103.
Hendry, J., Roscoe, W., Ross, D., 2006. Technical report on the Gatsuurt gold project, Northern Mongolia, prepared for Centerra Gold Inc. Roscoe Postle Associates Inc.,, Toronto, pp. 6–11.
Hodkiewicz, P., Groves, D., Davidson, G., Weinberg, R., Hagemann, S., 2009. Influence of structural setting on sulphur isotopes in Archean orogenic gold deposits, Eastern Goldfields Province, Yilgarn Western Australia. Miner. Depos. 44 (2), 129.
Hoefs, J., 2018. Stable Isotope Geochemistry. Springer.
Hou, L., Peng, H., Ding, J., Zhang, J., Zhu, S., Wu, S., Wu, Y., Ouyang, H., 2016. Textures and in situ chemical and isotopic analyses of pyrite, Huijiabao Trend, Youjiang Basin, China: implications for paragenesis and source of sulfur. Econ. Geol. 111 (2), 331–353.
Hou, W.-R., Nie, F.-J., Jiang, S.-H., Bai, D.-M., Liu, Y., Yun, F., Liu, Y.-F., 2010. SHRIMP zircon U-Pb dating of ore-bearing granite in the boroo large-size gold deposit, Mongolia and its geological significance. Diqiu Xuebao (Acta Geosci. Sin.) 31 (3), 331–342.
Kampe, A., Gottesmann, V., 1966. Report on Results of 1:50000 Scale Geological Mapping and General Prospecting Carried out in South-Western Khentii Gold-Bearing District. Geological Information Center, Ulaanbaatar Report No. 1836, (in Russian).
Kelty, T.K., Yin, A., Dash, B., Gehrels, G.E., Ribeiro, A.E., 2008. Detrital-zircon geochronology of Paleozoic sedimentary rocks in the Hangay-Hentey basin, north-central Mongolia: implications for the tectonic evolution of the Mongol-Okhotsk Ocean in central Asia. Tectonophysics 451 (1–4), 290–311.
Kerrich, R. (1987). The stable isotope geochemistry of Au-Ag vein deposits in metamorphic rocks. Mineral. Assoc. Canada, Short Course Handbook, 13, pp. 287–336.
Kerrich, R., 1989. Geochemical evidence on the sources of fluids and solutes for shear zone hosted mesothermal Au deposits. Miner. Shear Zones Geol. Assoc. Can. Short Course Notes 6, 129–197.
Khishgee, C., 2015. Orogenic Type Gold Mineralization in the North Khentei Gold belt, Central Northern Mongolia. Doctoral. Simane University, Matsue, Japan.
Khishgee, C., Akasaka, M., 2015. Mineralogy of the Boroo Gold Deposit in the North Khentei Gold Belt Central Northern Mongolia. Resour. Geol. 65 (4), 311–327.
Khishgee, C., Akasaka, M., Ohira, H., Sereenen, J., 2014. Gold mineralization of the G atsuurt deposit in the N orth K hentei gold belt, central N orthern M ongolia. Resour. Geol. 64 (1), 1–16.
Kim, N.K., Kusakabe, M., Park, C., Lee, J.I., Nagao, K., Enokido, Y., Yamashita, S., Park, S.Y., 2019. An automated laser fluorination technique for high precision analysis of three oxygen isotopes in silicates. Rapid Commnu. Mass Spectrom. 33, 641–649.
Koglin, N., Frimmel, H.E., Minter, W.L., Brätz, H., 2010. Trace-element characteristics of different pyrite types in Mesoarchaean to Palaeoproterozoic placer deposits. Miner. Depos. 45 (3), 259–280.
Koh, Y.-K., Choi, S.-G., So, C.-S., Choi, S.-H., Uchida, E., 1992. Application of arsenopyrite geothermometry and sphalerite geobarometry to the Taebaek Pb-Zn (-Ag) deposit at Yeonhwa I Mine, Republic of Korea. Miner. Depos. 27 (1), 58–65.
Kotlyar, B., Drown, T., Tungalag, F., Gantstetseg, O., 1998. Two types of mineralization in the north Khentei gold trend. Mongolian Geosci. 11, 10–13.
Kotlyar, B., Gantsetseg, O., Tungalag, F., Burentugs, J., 1999. Location and variations in mesothermal Au mineralization in the North Khentei gold trend. Mongolian Geosci. 14, 107–110.
Kretschmar, U., Scott, S., 1976. Phase relations involving arsenopyrite in the system Fe-As-S and their application. Can. Mineral. 14 (3), 364–386.
Krouse, H.R., Mayer, B., 2000. Sulphur and oxygen isotopes in sulphate. In: Environmental Tracers in Subsurface Hydrology. Springer, pp. 195–231.
LaFlamme, C., Jamieson, J.W., Fiorentini, M.L., Thébaud, N., Caruso, S., Selvaraja, V., 2018a. Investigating sulfur pathways through the lithosphere by tracing mass independent fractionation of sulfur to the Lady Bountiful orogenic gold deposit, Yilgarn

Craton. Gondwana Res.
LaFlamme, C., Sugiono, D., Thébaud, N., Caruso, S., Fiorentini, M., Selvaraja, V., Jeon, H., Voute, F., Martin, L., 2018b. Multiple sulfur isotopes monitor fluid evolution of an Archean orogenic gold deposit. Geochim. Cosmochim. Acta 222, 436–446.
Li, S.-R., Santosh, M., Zhang, H.-F., Luo, J.-Y., Zhang, J.-Q., Li, C.-L., Song, J.-Y., Zhang, X.-B., 2014. Metallogeny in response to lithospheric thinning and craton destruction: geochemistry and U-Pb zircon chronology of the Yixingzhai gold deposit, central North China Craton. Ore Geol. Rev. 56, 457–471.
Ma, Y., Jiang, S.-Y., Li, H.-L., 2018. Isotope geochemistry and genesis of the Liyuan gold deposit, Shanxi, North China. Ore Geol. Rev. 92, 129–143.
Mango, H., Ryan, P., 2015. Source of arsenic-bearing pyrite in southwestern Vermont, USA: sulfur isotope evidence. Sci. Total Environ. 505, 1331–1339.
McCuaig, T.C., Kerrich, R., 1998. P—T—t—deformation—fluid characteristics of lode gold deposits: evidence from alteration systematics. Ore Geol. Rev. 12 (6), 381–453.
Nesbitt, B., 1991. Phanerozoic gold deposits in tectonically active continental margins. In: Gold Metallogeny and Exploration. Springer, pp. 104–132.
Neumayr, P., Walshe, J., Hagemann, S., Petersen, K., Roache, A., Frikken, P., Horn, L., Halley, S., 2008. Oxidized and reduced mineral assemblages in greenstone belt rocks of the St. Ives gold camp, Western Australia: vectors to high-grade ore bodies in Archaean gold deposits? Miner. Depos. 43 (3), 363–371.
Niu, S.-D., Li, S.-R., Santosh, M., Zhang, D.-H., Li, Z.-D., Shan, M.-J., Lan, Y.-X., Gao, D.-R., Zhao, W.-B., 2016. Mineralogical and isotopic studies of base metal sulfides from the Jiawula Ag–Pb–Zn deposit, Inner Mongolia, NE China. J. Asian Earth Sci. 115, 480–491.
Ohmoto, H., 1972. Systematics of sulfur and carbon isotopes in hydrothermal ore deposits. Econ. Geol. 67 (5), 551–578.
Ohmoto, H., Rye, R.O., 1979. Isotopes of Sulfur and Carbon (H. Barnes Ed.). Wiley, New York.
Onon, G., Tsukada, K., 2017. Late Paleozoic low-angle southward-dipping thrust in the Züünharaa area, Mongolia: tectonic implications for the geological structures in the Sayan-Baikal and Hangai-Daur belts. Int. J. Earth Sci. 106 (7), 2549–2573.
Palin, J., Xu, Y., 2000. Gilt by association? Origins of pyritic gold ores in the Victory mesothermal gold deposit, Western Australia. Econ. Geol. 95 (8), 1627–1634.
Parfenov, L., Popeko, L., Tomurtogoo, O., 2001. Problems of tectonics of the Mongol-Okhotsk orogenic belt. Russ. J. Pacific Geol. 16 (5), 797–830.
Phillips, G., Powell, R., 2010. Formation of gold deposits: a metamorphic devolatilization model. J. Metamorph. Geol. 28 (6), 689–718.
Phillips, G.N., Groves, D.I., 1983. The nature of Archaean gold-bearing fluids as deduced from gold deposits of Western Australia. J. Geol. Soc. Aust. 30 (1–2), 25–39.
Phillips, G.N., Groves, D.I., Neall, F., Donnelly, T., Lambert, I., 1986. Anomalous sulfur isotope compositions in the Golden Mile Kalgoorlie. Econ. Geol. 81 (8), 2008–2015.
Pokrovski, G.S., Kokh, M.A., Guillaume, D., Borisova, A.Y., Gisquet, P., Hazemann, J.-L., Lahera, E., Del Net, W., Proux, O., Testemale, D., 2015. Sulfur radical species form gold deposits on Earth. Proc. Natl. Acad. Sci. 112 (44), 13484–13489.
Reich, M., Kesler, S.E., Utsunomiya, S., Palenik, C.S., Chryssoulis, S.L., Ewing, R.C., 2005. Solubility of gold in arsenian pyrite. Geochim. Cosmochim. Acta 69 (11), 2781–2796.
Ridley, J., Diamond, L., 2000. Fluid chemistry of orogenic lode gold deposits and implications for genetic models. Rev. Econ. Geol. 13, 141–162.
Rye, R.O., 2005. A review of the stable-isotope geochemistry of sulfate minerals in selected igneous environments and related hydrothermal systems. Chem. Geol. 215 (1–4), 5–36.
Seal, R.R., 2006. Sulfur isotope geochemistry of sulfide minerals. Rev. Mineral. Geochem. 61 (1), 633–677.
Sengor, A., Natal'In, B., 1996. Paleotectonics of Asia: fragments of a synthesis. In: Yin, A., Harrison, M. (Eds.), The Tectonic Evolution of Asia. Cambridge University Press, Cambridge, pp. 486–640.
Şengör, A., Natal'In, B., Burtman, V., 1993. Evolution of the Altaid tectonic collage and Palaeozoic crustal growth in Eurasia. Nature 364 (6435), 299.
Seward, T., 1993. The hydrothermal geochemistry of gold. In: Gold Metallogeny and Exploration. Springer, pp. 37–62.
Sheppard, S.M., 1986. Characterization and isotopic variations in natural waters. Rev. Mineral. Geochem. 16 (1), 165–183.
Simon, G., Kesler, S.E., Chryssoulis, S., 1999. Geochemistry and textures of gold-bearing arsenian pyrite, Twin Creeks, Nevada; implications for deposition of gold in Carlin-type deposits. Econ. Geol. 94 (3), 405–421.
Su, W., Xia, B., Zhang, H., Zhang, X., Hu, R., 2008. Visible gold in arsenian pyrite at the Shuiyindong Carlin-type gold deposit, Guizhou, China: implications for the environment and processes of ore formation. Ore Geol. Rev. 33 (3–4), 667–679.
Sung, Y.-H., Brugger, J., Ciobanu, C., Pring, A., Skinner, W., Nugus, M., 2009. Invisible gold in arsenian pyrite and arsenopyrite from a multistage Archaean gold deposit: sunrise Dam, Eastern Goldfields Province Western Australia. Miner. Depos. 44 (7), 765.
Taylor, B. (1987). Stable isotope geochemistry of oreforming fluids. Short course in stable isotope geochemistry of low temperature fluids, pp. 337–445.
Tomurtogoo, O., Windley, B., Kröner, A., Badarch, G., Liu, D., 2005. Zircon age and occurrence of the Adaatsag ophiolite and Muron shear zone, central Mongolia: constraints on the evolution of the Mongol-Okhotsk ocean, suture and orogen. J. Geol. Soc. 162 (1), 125–134.
Tumur, S., Lkhagvasuren, J., & Gerelmaa, N. (1995). Report of 1: 50000 scale geological mapping and general prospecting carried out in the Noyon Uul Area of the Boroo and Zuunmod District. Geological Information Center, Ulaanbaatar, Report(4859)((in Mongolian)).
Uemoto, T., Ridley, J., Mikucki, E., Groves, D.I., Kusakabe, M., 2002. Fluid chemical evolution as a factor in controlling the distribution of gold at the Archean Golden Crown lode gold deposit, Murchison province, Western Australia. Econ. Geol. 97 (6), 1227–1248.
Vallance, J., Boiron, M.-C., Cathelineau, M., Fourcade, S., Varlet, M., Marignac, C., 2004. The granite hosted gold deposit of Moulin de Cheni (Saint-Yrieix district, Massif Central, France): petrographic, structural, fluid inclusion and oxygen isotope constraints. Miner. Depos. 39 (3), 265–281.
Ward, J., Mavrogenes, J., Murray, A., Holden, P., 2017. Trace element and sulfur isotopic evidence for redox changes during formation of the Wallaby Gold Deposit, Western Australia. Ore Geol. Rev. 82, 31–48.
Wen, B.-J., Fan, H.-R., Santosh, M., Hu, F.-F., Pirajno, F., Yang, K.-F., 2015. Genesis of two different types of gold mineralization in the Linglong gold field, China: constrains from geology, fluid inclusions and stable isotope. Ore Geol. Rev. 65, 643–658.
Xu, D., Deng, T., Chi, G., Wang, Z., Zou, F., Zhang, J., Zou, S., 2017. Gold mineralization in the Jiangnan Orogenic Belt of South China: geological, geochemical and geochronological characteristics, ore deposit-type and geodynamic setting. Ore Geol. Rev. 88, 565–618.
Yakubchuk, A., Shatov, V., Kirwin, D., Edwards, A., Tomurtogoo, O., Badarch, G., & Buryak, V. (2005). Gold and Base Metal Metallogeny of the Central Asian Orogenic Supercollage: (Vol. Economic Geology, 100th Anniversary Volume, pp. 1035-1068).
Yuan, M.-W., Li, S.-R., Li, C.-L., Santosh, M., Alam, M., Zeng, Y.-J., 2018. Geochemical and isotopic composition of auriferous pyrite from the Yongxin gold deposit, Central Asian Orogenic Belt: implication for ore genesis. Ore Geol. Rev. 93, 255–267.
Zhang, L., Yang, L.-Q., Groves, D.I., Liu, Y., Sun, S.-C., Qi, P., Wu, S.-G., Peng, J.-S., 2018. Geological and H-O–S–Pb isotopic constraints on ore genesis, Huangjindong gold deposit, Jiangnan Orogen, southern China. Ore Geol. Rev.
Zhu, Y., An, F., Tan, J., 2011. Geochemistry of hydrothermal gold deposits: a review. Geosci. Front. 2 (3), 367–374.
Zoheir, B.A., 2008. Structural controls, temperature–pressure conditions and fluid evolution of orogenic gold mineralisation at the Betam mine, south Eastern Desert, Egypt. Miner. Depos. 43 (1), 79–95.
Zonenshain, L., Kuzmin, M., & Natapov, L. (1990). Geology of the USSR: A Plate-Tectonic Synthesis, Geodyn. Paper presented at the Ser.
Zorin, Y.A., 1999. Geodynamics of the western part of the Mongolia-Okhotsk collisional belt, Trans-Baikal region (Russia) and Mongolia. Tectonophysics 306 (1), 33–56.